WCAP-10786

ANALYSIS OF CAPSULE U FROM THE DUKE POWER COMPANY MCGUIRE UNIT 1 REACTOR VESSEL RADIATION SURVEILLANCE PROGRAM

S. E. Yanichko
T. V. Congedo
W. T. Kaiser

February 1985

APPROVED: T A Meyer
T. A. Meyer, Manager
Structural Materials and Reliability Technology

Work performed under Shop Order No. DVFJ-106

Prepared by Westinghouse Electric Corporation for the Duke Power Company

WESTINGHOUSE ELECTRIC CORPORATION
Nuclear Energy Systems
P.O. Box 355
Pittsburgh, Pennsylvania 15230

8485B:1b-022585

PREFACE

This report has been technically reviewed and verified.

	Reviewer	
Sections 1 through 5, 7 and 8	R. S. Boggs	R S Boggs
Section 6	S. L. Anderson	S L Anderson
Appendix A	F. J. Witt	F J Witt

TABLE OF CONTENTS

LIST OF ILLUSTRATIONS

LIST OF ILLUSTRATIONS (Cont)

LIST OF ILLUSTRATIONS (Cont)

LIST OF TABLES

LIST OF TABLES (Cont)

SECTION 1
SUMMARY OF RESULTS

The analysis of the reactor vessel material contained in surveillance Capsule U, the first capsule to be removed from the McGuire Unit 1 reactor pressure vessel, led to the following conclusions.

- The capsule received an average fast neutron fluence (E > 1.0 Mev) of 4.14×10^{18} n/cm^2.

- Irradiation of the reactor vessel intermediate shell plate B5012-1 to 4.14×10^{18} n/cm^2 resulted in 30 and 50 ft-lb transition temperature increases of 50°F and 40°F, respectively, for specimens oriented normal to the principal rolling direction of the plate, and 30 and 50 ft-lb transition temperature increases of 45°F for specimens oriented parallel to the plate principal rolling direction.

- Weld metal irradiated to 4.14×10^{18} n/cm^2 resulted in 30 and 50 ft-lb transition temperature increases of 160°F and 170°F, respectively.

- Weld HAZ metal showed a 30°F and 50°F transition temperature increase of 90°F and 95°F, respectively, after irradiation to 4.14×10^{18} n/cm^2.

- Plate B5012-1, weld metal, and HAZ metal all showed upper shelf energy levels well above 50 ft-lb after irradiation to 4.14×10^{18} n/cm^2.

SECTION 2
INTRODUCTION

This report presents the results of the examination of Capsule U, the first capsule to be removed from the reactor in the continuing surveillance program which monitors the effects of neutron irradiation on the McGuire Unit 1 reactor pressure vessel materials under actual operating conditions.

The surveillance program for tne McGuire Unit 1 reactor pressure vessel materials was designed and recommended by the Westinghouse Electric Corporation. A description of the surveillance program and the preirradiation mechanical properties of the reactor vessel materials are presented by Davidson and Yanichko[1]. The surveillance program was planned to cover the 40-year design life of the reactor pressure vessel and was based on ASTM E-185-73, "Recommended Practice for Surveillance Tests for Nuclear Reactor Vessels"[2]. Westinghouse Nuclear Energy Systems personnel were contracted for the preparation of procedures for removing the capsule from the reactor and its shipment to the Westinghouse Research and Development Laboratory, where the postirradiation mechanical testing of the Charpy V-notch impact and tensile surveillance specimens were performed.

This report summarizes the testing of and the postirradiation data obtained from surveillance Capsule U removed from the McGuire Unit 1 reactor vessel and discusses the analysis of these data.

SECTION 3
BACKGROUND

The ability of the large steel pressure vessel containing the reactor core and its primary coolant to resist fracture constitutes an important factor in ensuring safety in the nuclear industry. The beltline region of the reactor pressure vessel is the most critical region of the vessel because it is subjected to significant fast neutron bombardment. The overall effects of fast neutron irradiation on the mechanical properties of low alloy, ferritic pressure vessel steels such as SA 533 Grade B Class 1 (base material of the McGuire Unit 1 reactor pressure vessel beltline) are well documented in the literature. Generally, low alloy ferritic materials show an increase in hardness and tensile properties and a decrease in ductility and toughness under certain conditions of irradiation.

A method for performing analyses to guard against fast fracture in reactor pressure vessels has been presented in "Protection Against Nonductile Failure," Appendix G to Section III of the ASME Boiler and Pressure Vessel Code. The method utilizes fracture mechanics concepts and is based on the reference nil ductility temperature (RT_{NDT}).

RT_{NDT} is deformed as the greater of either the drop weight nil-ductility transition temperature (NDTT per ASTM E-208) or the temperature 60°F less than the 50 ft-lb (and 35-mil lateral expansion) temperature as determined from Charpy specimens oriented normal (transverse) to the major working direction of the material. The RT_{NDT} of a given material is used to index that material to a reference stress intensity factor curve (K_{IR} curve) which appears in Appendix G of the ASME Code. The K_{IR} curve is a lower bound of dynamics, crack arrest, and static fracture toughness results obtained from several heats of pressure vessel steel. When a given material is indexed to the K_{IR} curve, allowable stress intensity factors can be obtained for this material as a function of temperature. Allowable operating limits can then be determined utilizing these allowable stress intensity factors.

RT_{NDT} and, in turn, the operating limits of nuclear power plants can be adjusted to account for the effects of radiation on the reactor vessel material properties. The radiation embrittlement of changes in mechanical properties of a given reactor pressure vessel steel can be monitored by a reactor surveillance program such as the McGuire Unit 1 Reactor Vessel Radiation Surveillance Program[1], in which a surveillance capsule is periodically removed from the operating nuclear reactor and the encapsulated specimens are tested. The increase in the average Charpy V-notch 30 ft-lb temperature (ΔRT_{NDT}) due to irradiation is added to the original RT_{NDT} to adjust the RT_{NDT} for radiation embrittlement. This adjusted RT_{NDT} (RT_{NDT} initial + Δ RT_{NDT}) is used to index the material to the K_{IR} curve and, in turn, to set operating limits for the nuclear power plant which take into account the effects of irradiation on the reactor vessel materials.

SECTION 4
DESCRIPTION OF PROGRAM

Six surveillance capsules for monitoring the effects of neutron exposure on the McGuire Unit 1 reactor pressure vessel core region material were inserted in the reactor vessel prior to initial plant startup. The six capsules were positioned in the reactor vessel between the neutron shielding pads and the vessel wall as shown in figure 4-1. The vertical center of the capsules is opposite the vertical center of the core.

Capsule U was removed from the reactor after 1.06 Effective Full Power Years (EFPY) of plant operation. This capsule contained Charpy V-notch, tensile, and Compact Tension (CT) specimens from submerged arc weld metal representative of the reactor vessel core region weld metal, and Charpy V-notch, tensile, CT, and bend bar specimens from the intermediate shell plate B5012-1. The capsule also contained Charpy V-notch specimens from weld Heat Affected Zone (HAZ) metal. All heat affected zone specimens were obtained from the weld HAZ of plate B5012-1. The chemistry and heat treatment of the program surveillance materials is presented in table 4-1.

All test specimens were machined from the 1/4-thickness location of the plate. Test specimens represent material taken at least one-plate thickness from the quenched end of the plate. Some base metal Charpy V-notch and tensile specimens were oriented with the longitudinal axis of the specimens normal to (transverse orientation) and some parallel to (longitudinal orientation) the major working direction of the plate. The CT test specimens were machined so that the crack of the specimen would propagate normal to (longitudinal specimens) and parallel to (transverse specimens) the major working direction of the plate. All specimens were fatigue precracked per ASTM E399-72. The precracked bend bar was machined in the transverse orientation. Charpy V-notch specimens from the weld metal were oriented with the longitudinal axis of the specimens normal to (transverse orientation) the weld direction. Tensile specimens were oriented with the longitudinal axis of the specimens normal to (transverse orientation) the weld direction.

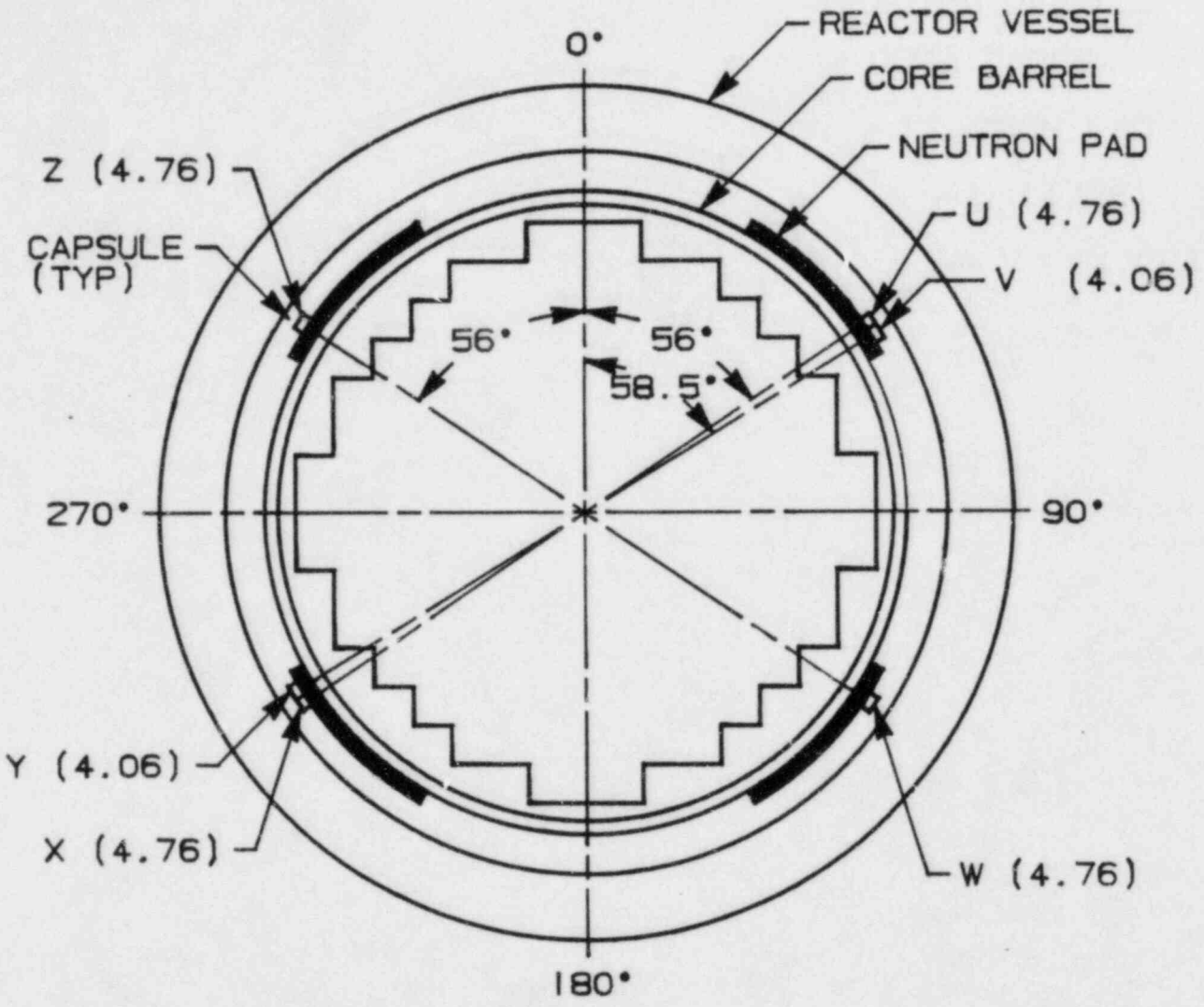

Figure 4-1. Arrangement of Surveillance Capsules in McGuire Unit 1 Reactor Vessel (Updated Lead Factors for the Capsules Shown in Parentheses)

TABLE 4-1

CHEMICAL COMPOSITION AND HEAT TREATMENT OF THE

MCGUIRE UNIT 1 REACTOR VESSEL SURVEILLANCE MATERIALS

Chemical Composition (wt%)

Element	Plate B5012-1	Weld Material	
C	0.21	0.10	
Mn	1.26	1.36	1.19[a]
P	0.010	0.011	0.010[a]
S	0.016	0.008	--
Si	0.23	0.24	0.23[a]
Cr	0.068	0.04	0.05[a]
Mo	0.57	0.55	0.54[a]
Ni	0.60	0.88	0.91[a]
Cu	0.087	0.21	0.20[a]
V	0.003	0.04	--
Sn	0.007	0.007	--
B	<0.003	<0.001	--
Cb	<0.001	<0.010	--
Ti	0.005	<0.010	--
W	<0.001	<0.010	--
As	0.008	0.009	--
Zr	0.003	<0.001	--
Sb	<0.001	0.002	--
Pb	0.001	<0.001	--
N_2	0.003	0.008	--
Co	0.016	0.014	--

Heat Treatment History

Material	Temperature (°F)	Time (Hr)	Coolant
Shell Plate B5012-1	1550-1650	4	Water quenched
	1200-1250	4	Air cooled
	1125-1175	40	Furnace cooled
Weld	1125-1175	40	Furnace cooled

a. Analysis performed on irradiated Charpy specimen DW-15

Capsule U contained dosimeter wires of pure copper, iron, nickel, and aluminum-0.15% cobalt (cadmium-shielded and unshielded). In addition, cadmium shielded dosimeters of Np^{237} and U^{238} were contained in the capsule.

Thermal monitors made from two low-melting eutectic alloys and sealed in Pyrex tubes were included in the capsule. The composition of the two alloys and their melting points are as follows.

2.5% Ag, 97.5% Pb	Melting point: 579°F (304°C)
1.75% Ag, 0.75% Sn, 97.5% Pb	Melting point: 590°F (312°C)

The arrangement of the various mechanical specimens, dosimeters and thermal monitors contained in Capsule U are shown in figure 4-2.

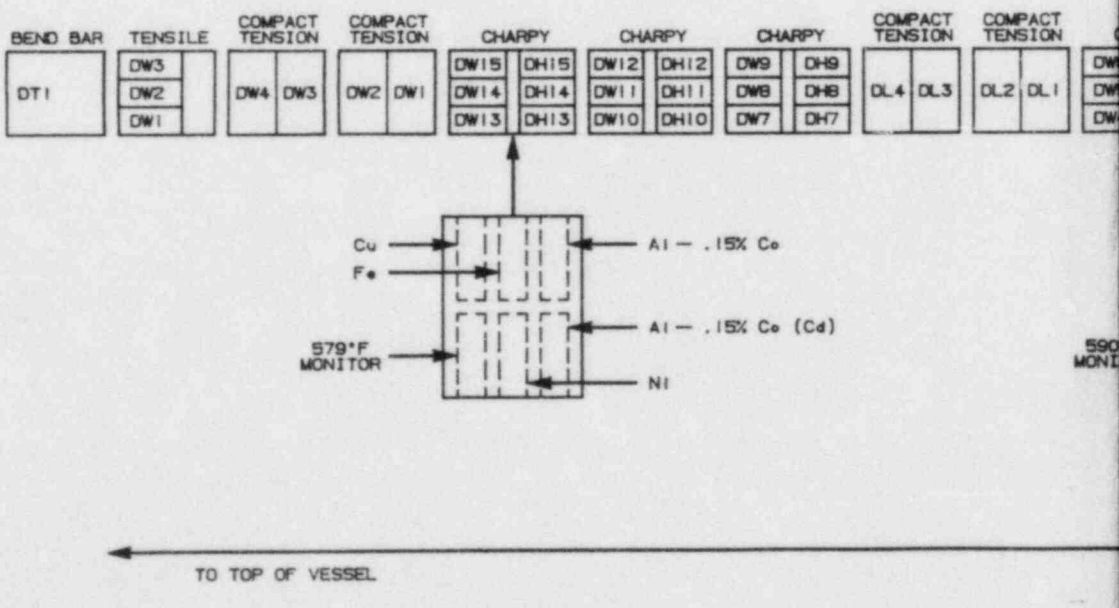
BEND BAR
TENSILE
COMPACT TENSION
COMPACT TENSION
CHARPY
CHARPY
CHARPY
COMPACT TENSION
COMPACT TENSION
DT1
DW3
DW2
DW1
DW4
DW3
DW2
DW1
DW15
DW14
DW13
DH15
DH14
DH13
DW12
DW11
DW10
DH12
DH11
DH10
DW9
DW8
DW7
DH9
DH8
DH7
DL4
DL3
DL2
DL1
Cu
Fe
579°F MONITOR
Al — .15% Co
Al — .15% Co (Cd)
Ni
TO TOP OF VESSEL

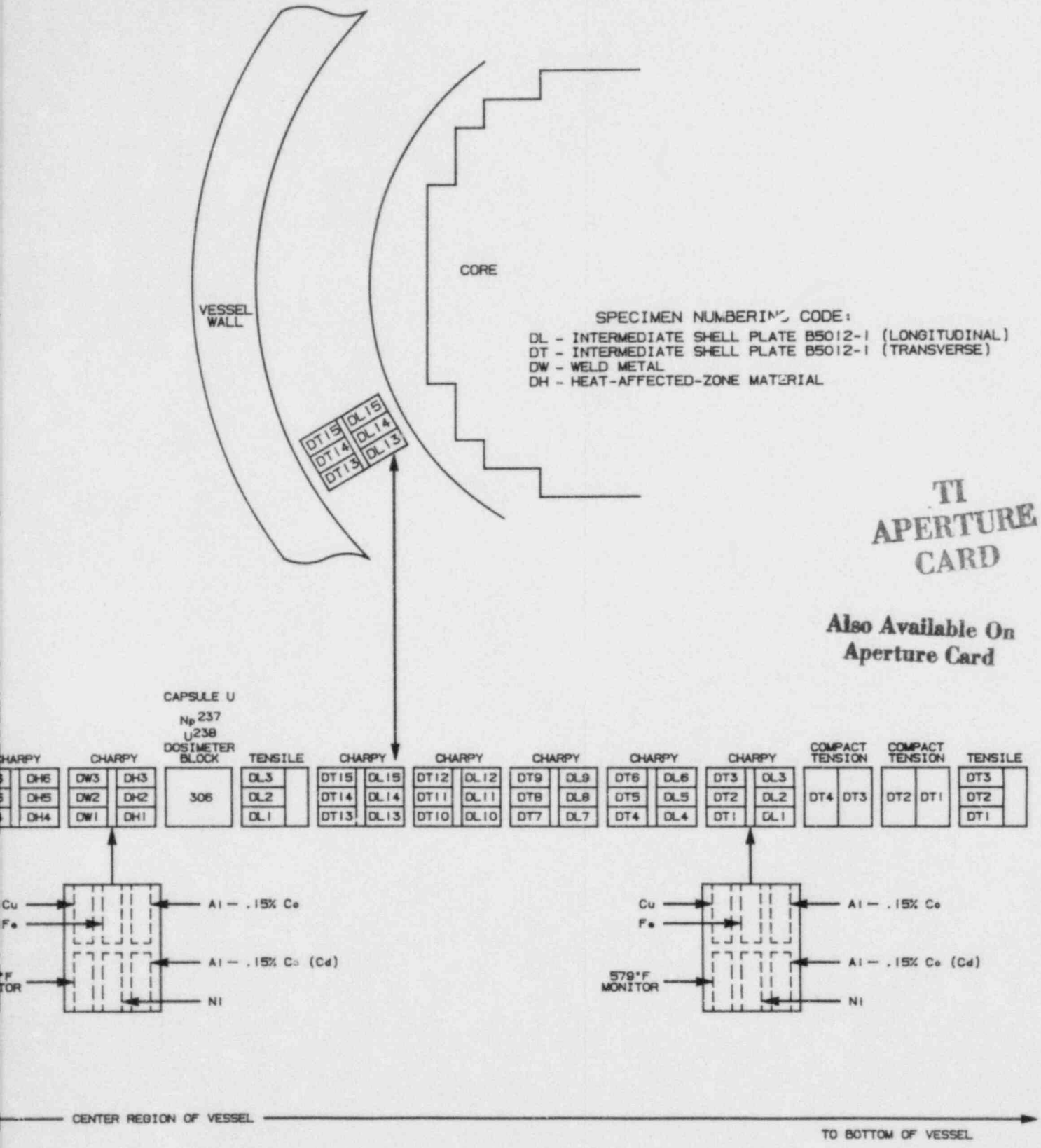

Figure 4-2. Capsule U Diagram Showing Location of Specimens, Thermal Monitors, and Dosimeters

SECTION 5
TESTING OF SPECIMENS FROM CAPSULE U

5.1. OVERVIEW

The postirradiation mechanical testing of the Charpy V-notch and tensile specimens was performed at the Westinghouse Research and Development Laboratory with consultation by Westinghouse Nuclear Energy Systems personnel. Testing was performed in accordance with 10CFR50, Appendices G and H, ASTM Specification E185-82, and Westinghouse Procedure RMF-8402, Revision 0.

Upon receipt of the capsule at the laboratory, the specimens and spacer blocks were carefully removed, inspected for identification number, and checked against the master list in WCAP-9195[1]. No discrepancies were found.

Examination of the two low-melting point 304°C (579°F) and 310°C (590°F) eutectic alloys indicated no melting of either type of thermal monitor. Based on this examination, the maximum temperature to which the test specimens were exposed was less than 304°C (579°F).

The Charpy impact tests were performed per ASTM Specification E23-82 and RMF Procedure 8103 on a Tinius-Olsen Model 74,358J machine. The tup (striker) of the Charpy machine is instrumented with an Effects Technology Model 500 instrumentation system. With this system, load-time and energy-time signals can be recorded in addition to the standard measurement of Charpy energy (E_D). From the load-time curve, the load of general yielding (P_{GY}), the time to general yielding (t_{GY}), the maximum load (P_M), and the time to maximum load (t_M) can be determined. Under some test conditions, a sharp drop in load indicative of fast fracture was observed. The load at which fast fracture was initiated is identified as the fast fracture load (P_F), and the load at which fast fracture terminated is identified as the arrest load (P_A).

The energy at maximum load (E_M) was determined by comparing the energy-time record and the load-time record. The energy at maximum load is roughly equivalent to the energy required to initiate a crack in the specimen.

Therefore, the propagation energy for the crack (E_p) is the difference between the total energy to fracture (E_D) and the energy at maximum load.

The yield stress (σy) is calculated from the three-point bend formula. The flow stress is calculated from the average of the yield and maximum loads, also using the three-point bend formula.

Percent shear was determined from postfracture photographs using the ratio-of-areas methods in compliance with ASTM Specification A370-77. The lateral expansion was measured using a dial gage rig similar to that shown in the same specification.

Tension tests were performed on a 20,000-pound Instron, split-console test machine (Model 1115) per ASTM Specifications E8-81 and E21-79, and RMF Procedure 8102. All pull rods, grips, and pins were made of Inconel 718 hardened to Rc 45. The upper pull rod was connected through a universal joint to improve axiality of loading. The tests were conducted at a constant crosshead speed of 0.05 inches per minute throughout the test.

Deflection measurements were made with a linear variable displacement transducer (LVDT) extensometer. The extensometer knife edges were spring-loaded to the specimen and operated through specimen failure. The extensometer gage length is 1.00 inch. The extensometer is rated as Class B-2 per ASTM E83-67.

Elevated test temperatures were obtained with a three-zone electric resistance split-tube furnace with a 9-inch hot zone. All tests were conducted in air.

Because of the difficulty in remotely attaching a thermocouple directly to the specimen, the following procedure was used to monitor specimen temperature. Chromel-alumel thermocouples were inserted in shallow holes in the center and each end of the gage section of a dummy specimen and in each grip. In the test configuration, with a slight load on the specimen, a plot of specimen temperature versus upper and lower grip and controller temperatures was developed over the range room temperature to 550°F (288°C). The upper grip was used to control the furnace temperature. During the actual testing the

grip temperatures were used to obtain desired specimen temperatures. Experiments indicated that this method is accurate to $\pm$2°F.

The yield load, ultimate load, fracture load, total elongation, and uniform elongation were determined directly from the load-extension curve. The yield strength, ultimate strength, and fracture strength were calculated using the original cross-sectional area. The final diameter and final gage length were determined from post-fracture photographs. The fracture area used to calculate the fracture stress (true stress at fracture) and percent reduction in area was computed using the final diameter measurement.

5-2. CHARPY V-NOTCH IMPACT TEST RESULTS

The results of Charpy V-notch impact tests performed on the various materials contained in Capsule U irradiated at 4.14×10^{18} n/cm^2 are presented in tables 5-1 through 5-5 and figures 5-1 through 5-4. The fractured surfaces of the impact specimens are shown in figures 5-5 through 5-8.

Irradiation of Charpy V-notch impact specimens from the reactor vessel intermediate shell plate, B5012-1, to 4.14×10^{18} n/cm^2 as shown in figure 5-1 resulted in 30 and 50 ft-lb transition temperature increases of 50°F and 40°F, respectively, for specimens oriented normal to the principal rolling direction (transverse orientation) of the plate. Specimens oriented parallel to the principal rolling direction (longitudinal orientation) of the plate as shown in figure 5-2 exhibited a transition temperature increase of 45°F at both the 30 and 50 ft-lb index temperatures. The upper shelf energy of the shell plate showed a 1 ft-lb decrease in the transverse direction and a 7 ft-lb decrease in the longitudinal direction.

Weld metal specimens irradiated to 4.14×10^{18} n/cm^2 resulted in 30 ft-lb and 50 ft-lb transition temperature increases of 160°F and 170°F, respectively, as shown in figure 5-3. Irradiation caused the upper shelf energy of the weld metal to decrease 37 ft-lb to a shelf energy level of 75 ft-lb. A comparison of the 30 ft-lb transition temperature increase shown in figure 5-9 with the predicted increase based on U.S. Nuclear Regulatory Commission Regulatory Guide 1.99, Revision 1[3] indicates that the weld metal is more sensitive than predicted at a fluence of 4.14×10^{18} n/cm^2.

TABLE 5-1

CHARPY V-NOTCH IMPACT DATA FOR THE MCGUIRE UNIT 1

INTERMEDIATE SHELL PLATE B5012-1

IRRADIATED AT 550°F, FLUENCE 4.14 x 10^{18} n/cm^2 (E > 1 Mev)

Sample No.	Temperature (°F)	(°C)	Impact Energy (ft-lb)	(J)	Lateral Expansion (mils)	(mm)	Shear (%)
			Longitudinal Orientation				
DL11	0	-18	17.0	23.0	14.5	0.37	1
DL10	50	10	23.0	31.0	21.5	0.55	23
DL5	50	10	35.0	47.5	29.5	0.75	22
DL6	76	24	78.0	106.0	52.5	1.33	39
DL14	76	24	55.0	74.5	42.5	1.08	30
DL2	76	24	45.0	61.0	33.5	0.85	31
DL4	100	38	54.0	73.0	46.0	1.17	32
DL1	100	38	78.0	106.0	58.5	1.49	48
DL7	125	52	82.0	111.0	61.0	1.55	54
DL12	150	66	109.0	148.0	78.0	1.98	69
DL9	200	93	119.0	161.5	81.0	2.06	85
DL15	250	121	135.0	183.0	87.5	2.22	100
DL3	300	149	133.0	180.5	84.0	2.13	100
DL8	400	204	130.0	176.5	79.0	2.01	100
			Transverse Orientation				
DT7	-50	-46	5.0	7.0	5.5	0.14	1
DT15	0	-18	8.0	11.0	7.5	0.19	5
DT13	25	-4	24.0	32.5	21.0	0.53	6
DT8	50	10	37.0	50.0	29.5	0.75	9
DT4	50	10	31.0	42.0	29.0	0.74	16
DT1	76	24	46.0	62.5	36.5	0.93	35
DT3	76	24	35.0	47.5	30.5	0.77	33
DT6	100	38	47.0	63.5	42.0	1.07	44
DT10	100	38	42.0	57.0	37.0	0.94	43
DT2	125	52	58.0	78.5	44.0	1.12	53
DT12	150	66	72.0	97.5	57.5	1.46	73
DT11	200	93	81.0	110.0	59.5	1.51	85
DT5	250	121	102.0	138.5	72.0	1.83	100
DT9	300	149	104.0	141.0	72.0	1.83	100
DT14	400	204	95.0	129.0	65.0	1.65	100

TABLE 5-2

CHARPY V-NOTCH IMPACT DATA FOR THE MCGUIRE UNIT 1

REACTOR VESSEL WELD METAL AND HAZ METAL

IRRADIATED AT 550°F, FLUENCE 4.14 x 10^{18} n/cm^2 (E > 1 Mev)

Sample No.	Temperature (°F)	(°C)	Impact Energy (ft-lb)	(J)	Lateral Expansion (mils)	(mm)	Shear (%)
			Weld Metal				
DW8	0	-18	4.0	5.5	5.0	0.13	4
DW12	76	24	12.0	16.5	11.0	0.28	19
DW11	120	49	24.0	32.5	22.5	0.57	27
DW4	140	60	35.0	47.5	33.0	0.84	35
DW15	150	66	33.0	44.5	32.0	0.81	49
DW6	150	66	36.0	49.0	33.0	0.84	51
DW9	175	79	31.0	42.0	30.5	0.77	54
DW10	175	79	34.0	46.0	33.5	0.85	67
DW13	200	93	37.0	50.0	36.0	0.91	75
DW5	220	104	68.0	92.0	55.5	1.41	87
DW2	220	104	71.0	96.5	60.0	1.52	98
DW1	250	121	71.0	96.5	61.5	1.56	98
DW14	300	149	71.0	96.5	71.5	1.82	98
DW7	400	204	79.0	107.0	68.5	1.74	100
DW3	450	232	78.0	106.0	69.5	1.77	100
			HAZ Metal				
DH1	-50	-46	7.0	9.5	9.0	0.23	2
DH9	0	-18	29.0	39.5	23.5	0.60	27
DH8	50	10	37.0	50.0	35.5	0.90	48
DH13	50	10	42.0	57.0	32.5	0.83	36
DH10	76	24	35.0	47.5	35.0	0.89	45
DH12	76	24	35.0	47.5	29.0	0.74	38
DH2	100	38	78.0	106.0	62.5	1.57	69
DH7	100	38	52.0	70.5	46.0	1.17	57
DH11	120	49	77.0	104.5	58.5	1.49	76
DH6	150	66	49.0	66.5	43.5	1.10	64
DH15	150	66	83.0	112.5	65.0	1.65	80
DH14	200	93	78.0	106.0	62.0	1.57	85
DH4	250	121	100.0	135.5	77.5	1.97	100
DH3	300	149	106.0	143.5	77.0	1.96	100
DH5	400	204	119.0	161.5	82.5	2.10	100

TABLE 5-3
INSTRUMENTED CHARPY IMPACT TEST RESULTS FOR MCGUIRE UNIT 1
INTERMEDIATE SHELL PLATE B5012-1 IRRADIATED
AT 4.14 x 10^{18} n/cm^2 (E > 1 Mev)

Sample Number	Test Temp (°F)	Charpy Energy (ft-lb)	Normalized Energies (ft-lb/in^2) Charpy Ed/A	Maximum Em/A	Prop Ep/A	Yield Load (kips)	Time to Yield (μsec)	Maximum Load (kips)	Time to Maximum (μsec)	Fracture Load (kips)	Arrest Load (kips)	Yield Stress (ksi)	Flow Stress (ksi)
Longitudinal Orientation													
DL11	0	17.0	137	110	27	3.35	110	3.90	295	3.80	--	111	120
DL5	50	35.0	282	214	68	3.05	90	4.15	505	4.10	--	100	119
DL10	50	23.0	185	120	65	3.15	90	3.75	310	3.75	0.40	104	114
DL2	76	45.0	362	208	154	2.75	75	3.95	505	3.80	1.60	90	111
DL6	76	78.0	628	365	263	2.85	80	4.25	815	4.05	1.30	95	117
DL14	76	55.0	443	289	154	3.00	90	4.25	655	4.20	1.35	100	120
DL1	100	78.0	628	332	296	2.85	85	4.10	770	3.75	1.20	94	115
DL4	100	54.0	435	327	108	2.85	95	4.05	770	4.05	1.10	95	114
DL7	125	82.0	660	269	392	2.70	80	3.95	650	3.50	1.85	90	110
DL12	150	109.0	878	319	559	2.75	85	4.05	755	3.15	1.80	91	112
DL9	200	119.0	958	268	690	2.60	80	3.95	655	2.55	2.25	86	108
DL15	250	135.0	1087	290	797	2.15	50	3.75	725	--	--	71	98
DL3	300	133.0	1071	255	816	2.30	80	3.65	665	--	--	76	98
DL8	400	130.0	1047	285	762	1.90	55	3.50	770	--	--	63	89
Transverse Orientation													
DT7	-50	5.0	40	25	15	2.80	70	3.40	95	3.40	0.15	92	102
DT15	0	8.0	64	39	25	3.10	85	3.45	130	3.45	0.15	102	108
DT13	25	24.0	193	146	48	3.10	85	4.00	355	3.80	--	103	118
DT8	50	37.0	298	219	79	3.10	95	4.25	510	4.20	--	103	122
DT4	50	31.0	250	185	65	3.00	80	4.10	435	4.05	--	99	117
DT1	76	46.0	370	241	130	2.80	75	4.10	560	3.80	1.15	92	114
DT3	76	35.0	282	172	110	3.15	90	4.10	410	4.00	0.90	104	120
DT6	100	47.0	378	211	168	2.90	85	4.05	505	3.90	1.10	96	115
DT10	100	42.0	338	202	136	2.85	80	4.00	485	4.00	1.65	95	114
DT2	125	58.0	467	241	226	2.70	75	4.05	570	3.85	1.70	88	111
DT12	150	72.0	580	277	303	2.85	85	4.10	650	3.65	2.15	93	114
DT11	200	81.0	652	270	383	2.65	85	3.95	655	3.85	2.80	87	109
DT5	250	102.0	821	253	568	2.25	55	3.80	630	--	--	74	100
DT9	300	104.0	837	247	591	2.20	65	3.70	640	--	--	72	97
DT14	400	95.0	765	211	554	2.15	60	3.50	570	--	--	71	93

TABLE 5-4
INSTRUMENTED CHARPY IMPACT TEST RESULTS FOR MCGUIRE UNIT 1
WELD METAL AND HAZ METAL IRRADIATED
AT 4.14 x 10^{18} n/cm^2 (E > 1 Mev)

Sample Number	Test Temp (°F)	Charpy Energy (ft-lb)	Normalized Energies (ft-lb/in^2) Charpy Ed/A	Maximum Em/A	Prop Ep/A	Yield Load (kips)	Time to Yield (μsec)	Maximum Load (kips)	Time to Maximum (μsec)	Fracture Load (kips)	Arrest Load (kips)	Yield Stress (ksi)	Flow Stress (ksi)
Weld Metal													
DW8	0	4.0	32	25	7	--	--	3.55	95	3.45	--	--	--
DW12	76	12.0	97	33	64	3.10	100	3.30	125	3.30	0.75	102	105
DW11	120	24.0	193	139	54	3.00	85	3.75	355	3.65	1.05	99	111
DW4	140	35.0	282	192	90	3.00	85	3.95	460	4.00	1.40	99	115
DW15	150	33.0	266	179	87	2.9	90	3.80	450	3.80	1.10	95	111
DW6	150	36.0	290	204	85	2.95	85	3.90	495	3.80	1.40	98	114
DW9	175	31.0	250	156	93	2.95	85	3.75	395	3.75	1.60	97	110
DW10	175	34.0	274	178	96	2.90	85	3.80	445	3.80	2.00	96	111
DW13	200	37.0	298	159	139	2.9	80	3.75	400	3.75	2.05	95	110
DW5	220	68.0	548	203	345	2.60	70	3.85	495	--	--	86	107
DW2	220	71.0	572	228	344	2.65	85	3.85	560	--	--	88	108
DW1	250	71.0	572	201	370	2.75	85	3.80	505	--	--	91	108
DW14	300	71.0	572	194	378	2.60	80	3.60	505	--	--	85	102
DW7	400	79.0	636	191	445	2.35	70	3.60	505	--	--	78	99
DW3	450	78.0	628	217	411	2.15	60	3.55	580	--	--	70	94
HAZ Metal													
DH1	-50	7.0	56	11	46	--	--	2.50	60	2.50	0.70	--	--
DH9	0	29.0	234	147	86	3.45	90	4.10	350	4.10	1.15	113	124
DH8	50	37.0	298	103	195	3.35	85	3.85	260	3.75	2.25	111	119
DH13	50	42.0	338	184	155	3.35	85	4.15	420	4.20	2.90	111	124
DH10	76	35.0	282	99	183	3.10	80	3.65	260	3.45	2.10	102	111
DH12	76	35.0	282	138	144	3.35	90	4.00	335	3.80	2.05	111	121
DH2	100	78.0	628	295	333	3.15	90	4.25	665	4.00	2.75	105	122
DH7	100	52.0	419	143	276	3.15	90	3.90	355	--	--	105	117
DH11	120	77.0	620	279	341	3.10	85	4.00	650	--	--	102	117
DH6	150	49.0	395	179	216	3.10	95	3.85	445	3.70	2.65	102	115
DH15	150	83.0	668	287	381	2.90	90	4.20	665	--	--	96	117
DH14	200	78.0	628	203	425	2.90	85	3.80	500	--	--	97	111
DH4	250	100.0	805	323	482	2.65	85	3.95	770	--	--	88	109
DH3	300	106.0	854	334	519	2.50	75	3.85	815	--	--	82	105
DH5	400	119.0	958	286	672	2.30	55	3.70	725	--	--	76	99

Material	Average 50 ft-lb Temperature (°F) Unirradiated	Irradiated	ΔT	La U
Plate B5012-1 (Transverse)	75	115	40	
Rate B5012-1 (Longitudinal)	35	80	45	
Weld metal	20	190	170	
HAZ metal	-5	90	95	

TABLE 5-5

CT OF 550°F IRRADIATION AT 4.14×10^{18} n/cm^2 (E > 1 Mev) ON NOTCH TOUGHNESS PROPERTIES OF MCGUIRE UNIT 1 REACTOR VESSEL MATERIALS

Average 35 mil Lateral Expansion Temperature (°F)			Average 30 ft-lb Temperature (°F)			Average Energy Absorbtion at Full Shear (ft-lb)		
Unirradiated	Irradiated	ΔT	Unirradiated	Irradiated	ΔT	Unirradiated	Irradiated	Δft lb
50	85	35	0	50	50	101	100	-1
35	70	35	5	50	45	140	133	-7
0	170	170	-5	155	160	112	75	-37
-15	70	85	-50	40	90	118	108	-10

12216-3

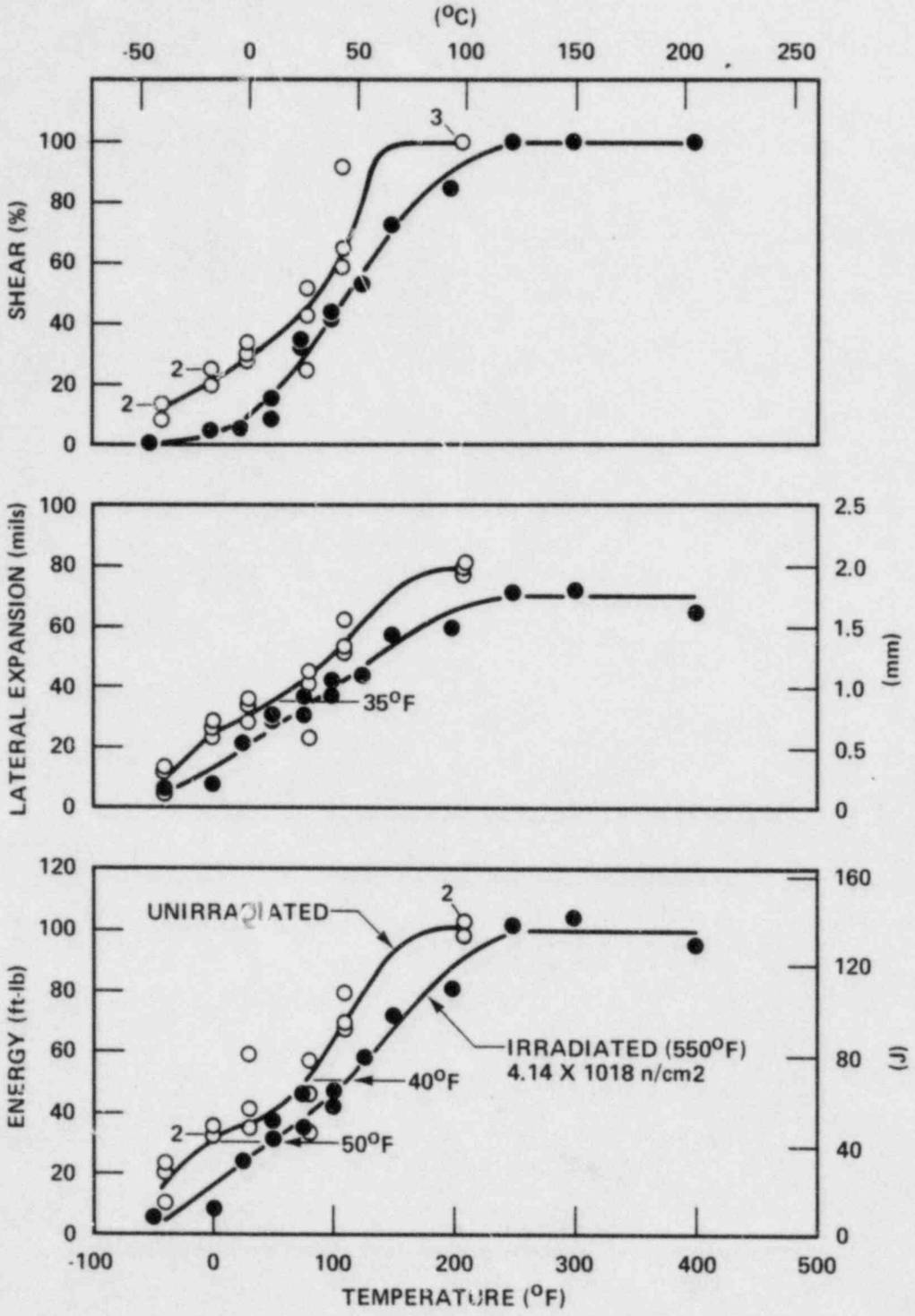

Figure 5-1. Charpy V-Notch Impact Data for McGuire Unit 1 Reactor Vessel Shell Plate B5012-1 (Transverse Orientation)

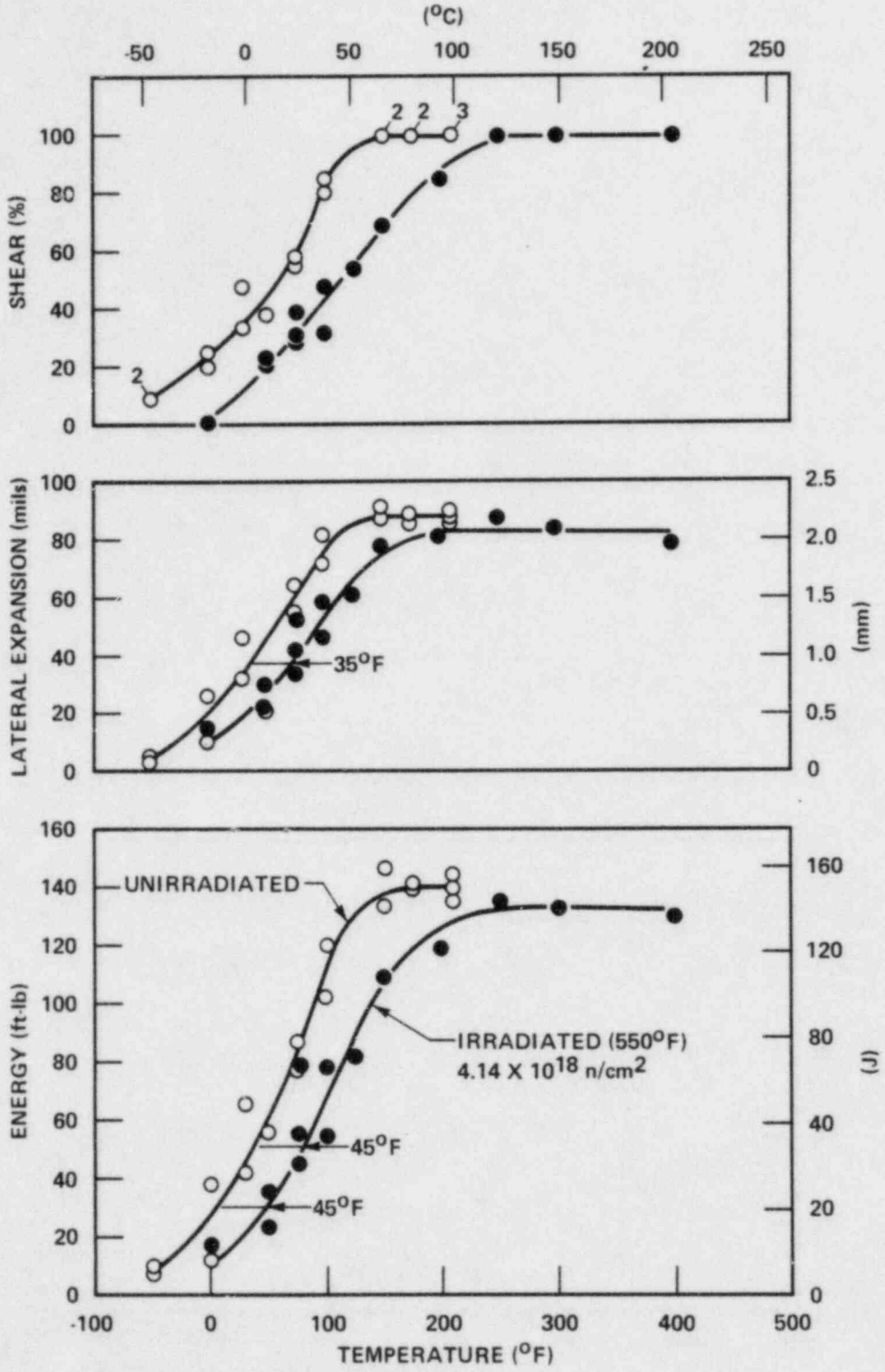

Figure 5-2. Charpy V-Notch Impact Data for McGuire Unit 1 Reactor Vessel Shell Plate B5012-1 (Longitudinal Orientation)

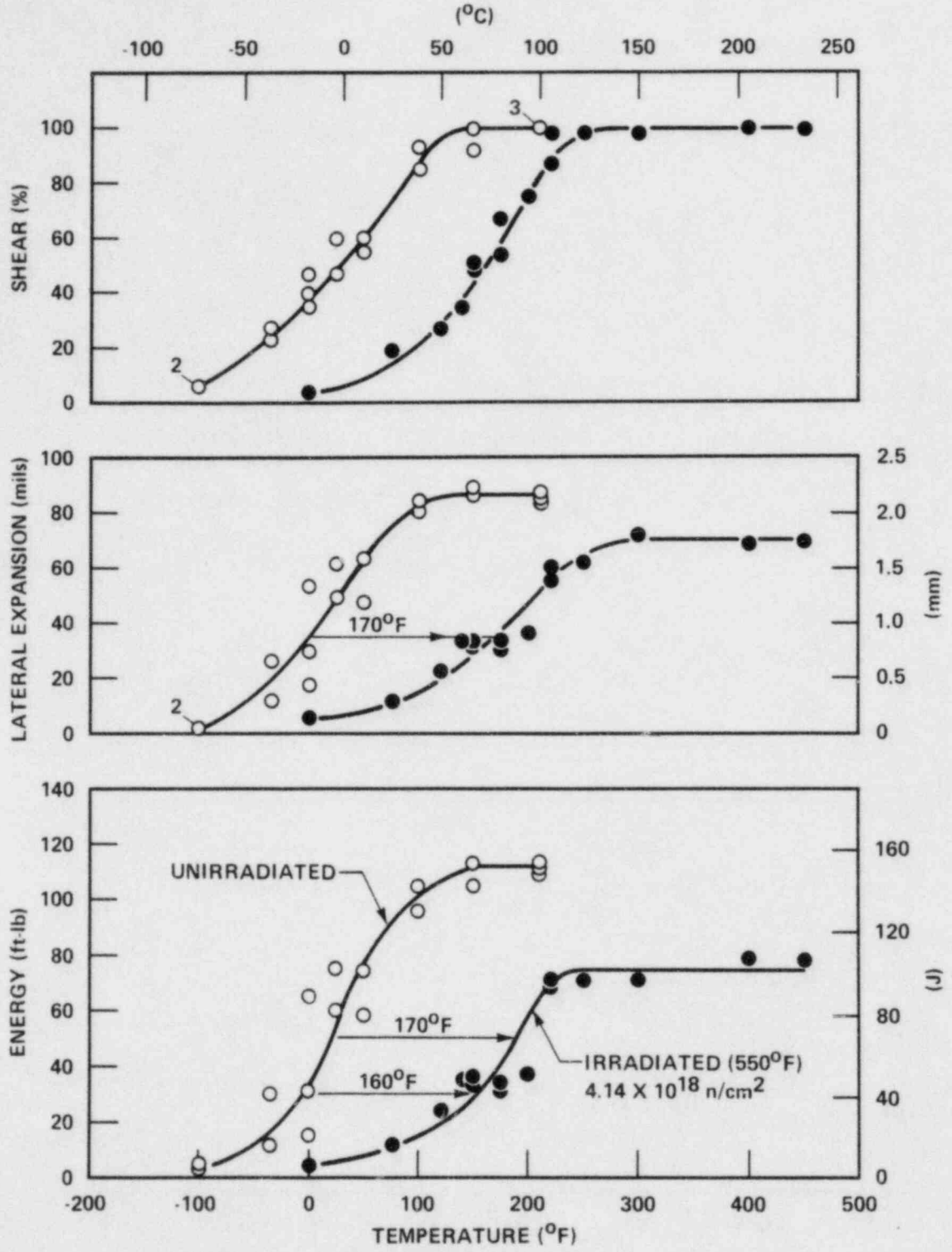

Figure 5-3. Charpy V-Notch Impact Data for McGuire Unit 1 Reactor Vessel Weld Metal

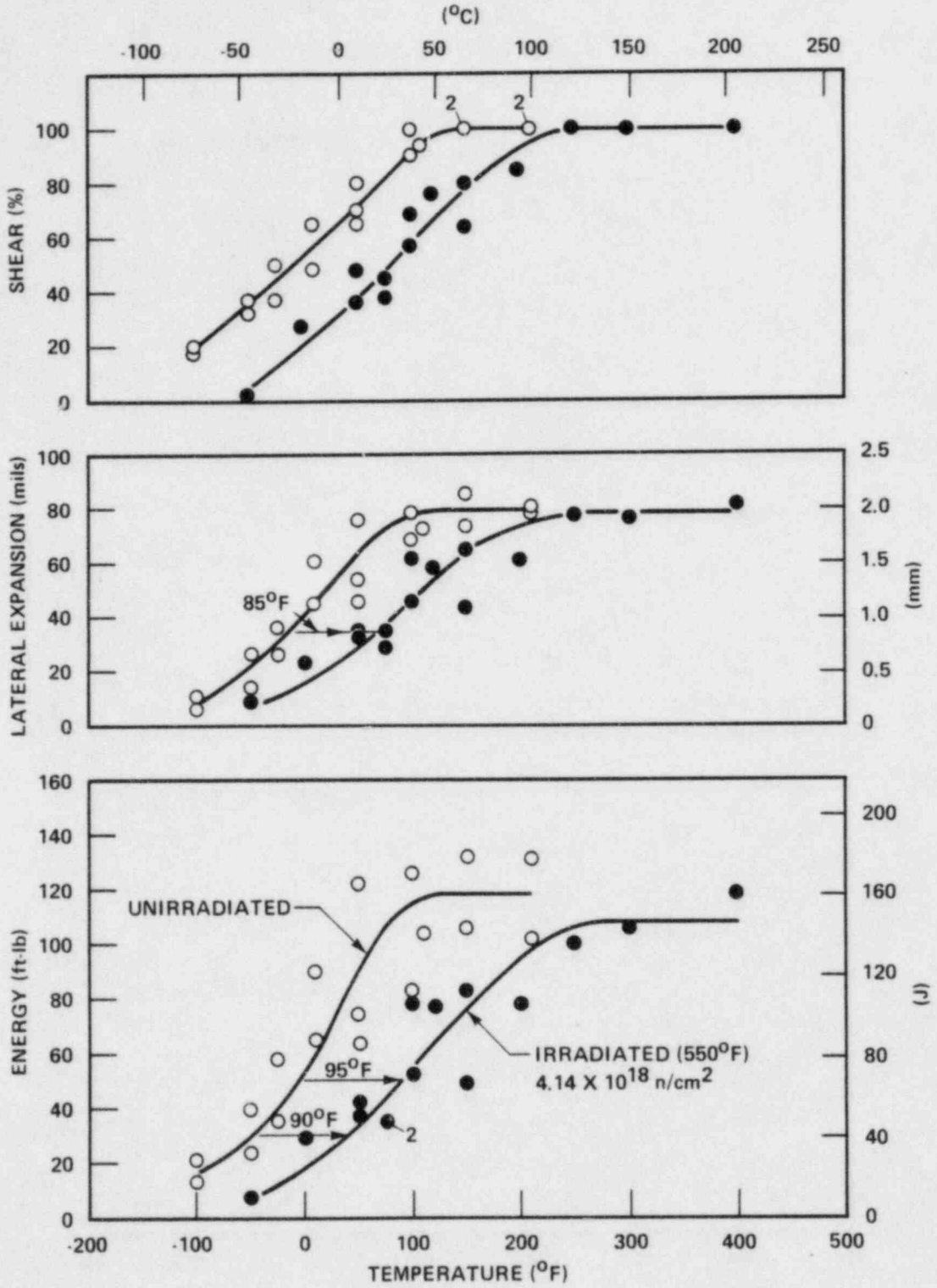

Figure 5-4. Charpy V-Notch Impact Data for McGuire Unit 1 Reactor Vessel Weld HAZ Metal

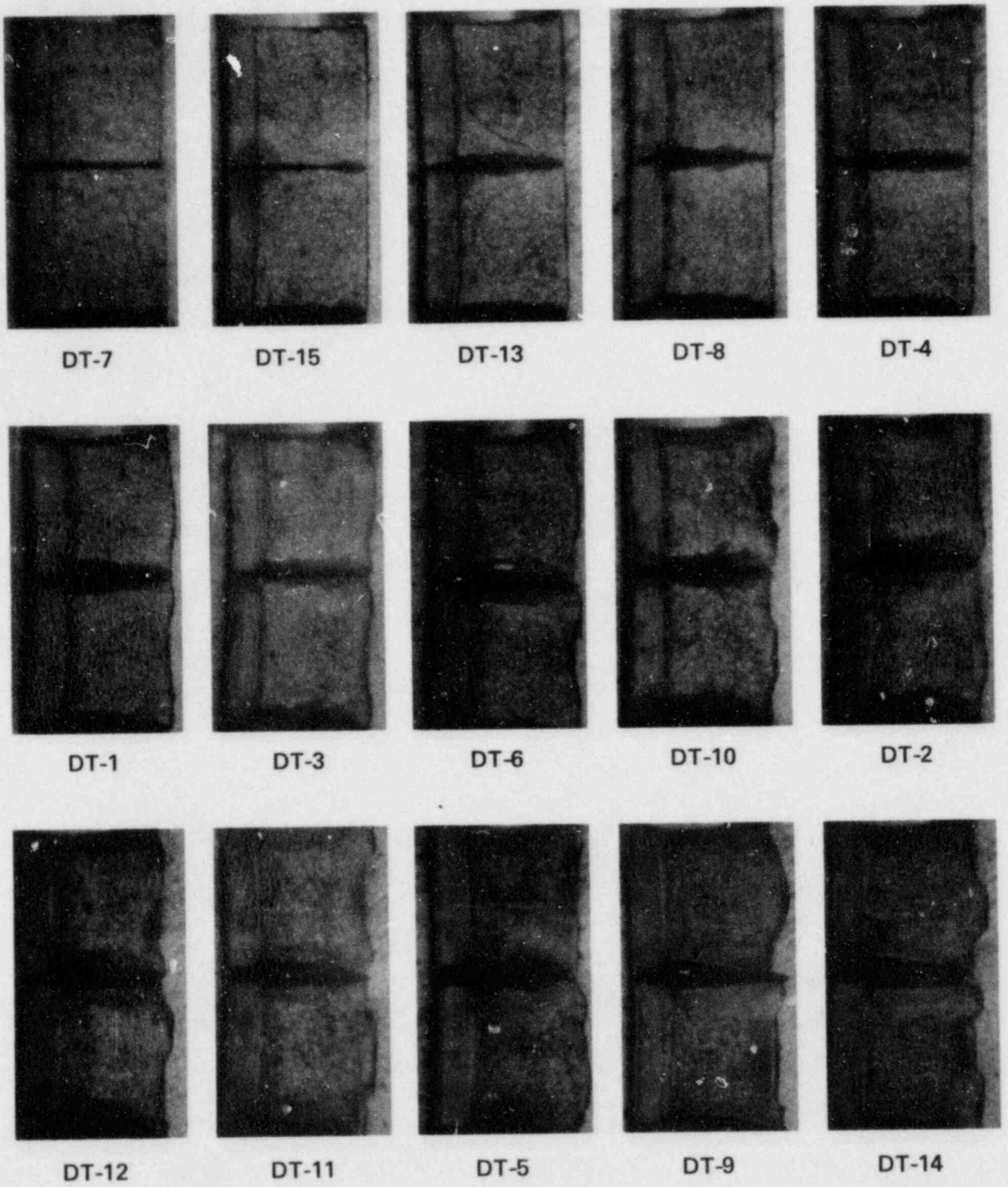

Figure 5-5. Charpy Impact Specimen Fracture Surfaces for McGuire Unit 1 Reactor Vessel Shell Plate B5012-1 (Transverse Orientation)

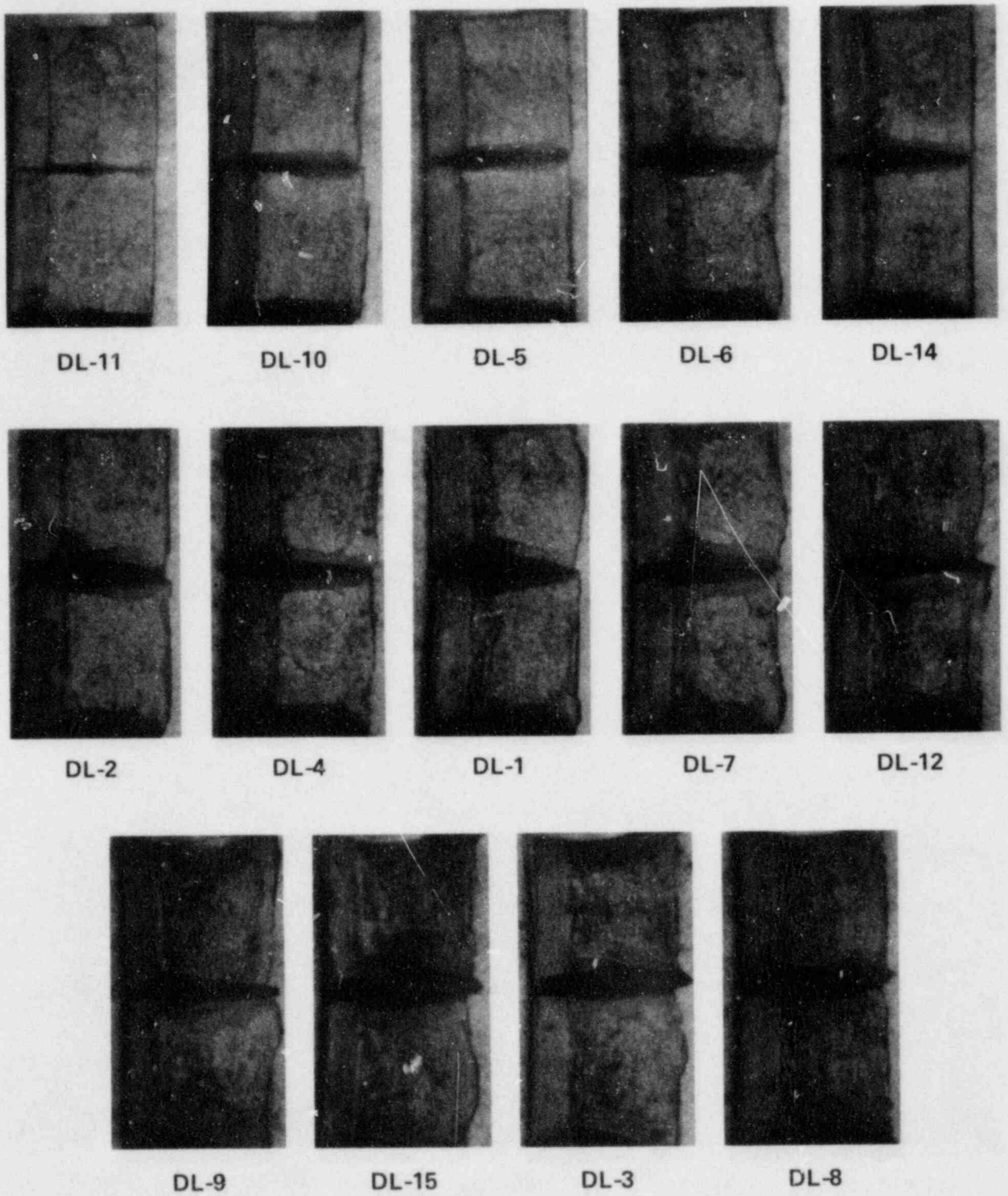

Figure 5-6. Charpy Impact Specimen Fracture Surfaces for McGuire Unit 1 Reactor Vessel Shell Plate B5012-1 (Longitudinal Orientation)

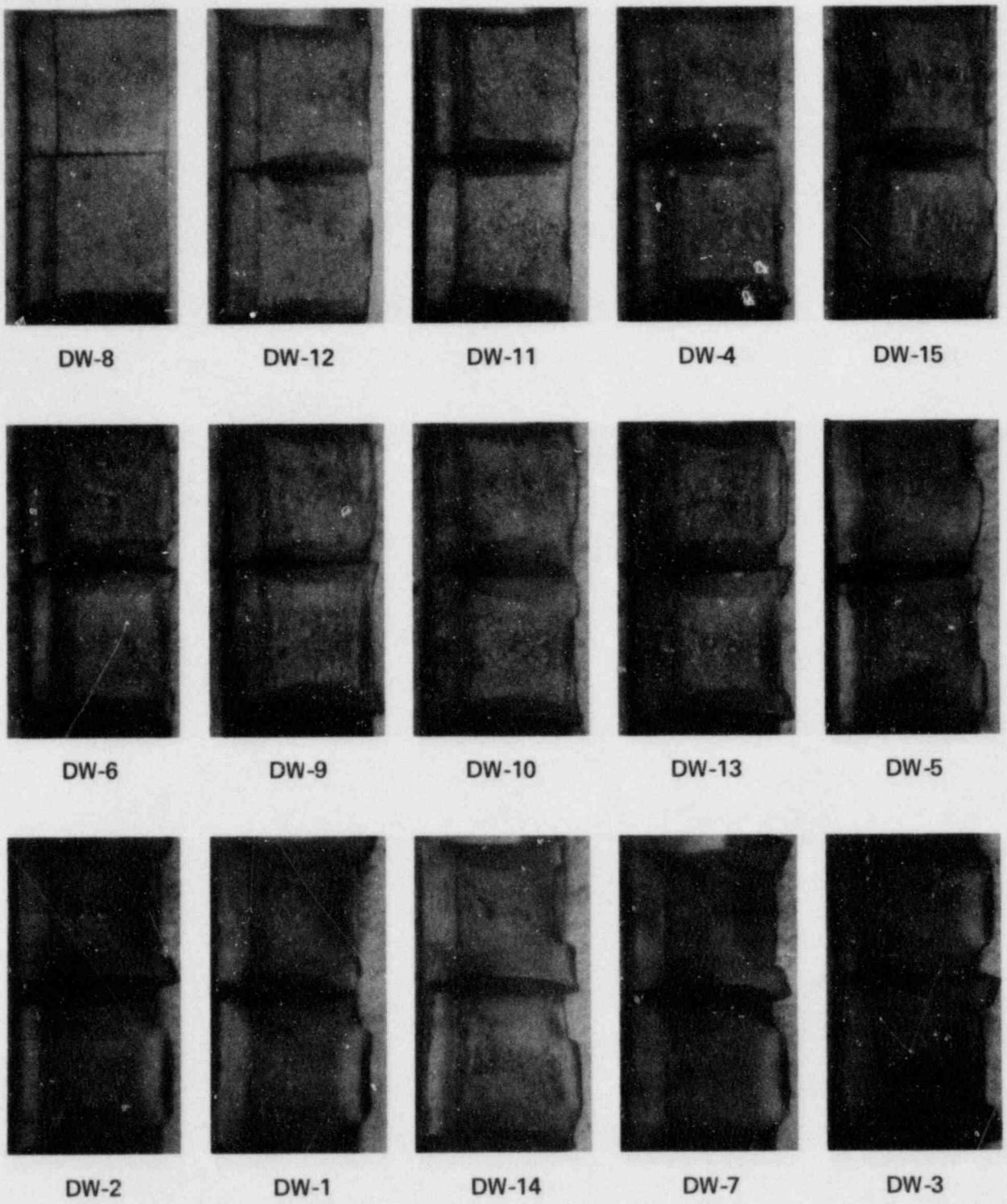

Figure 5-7. Charpy Impact Specimen Fracture Surfaces for McGuire Unit 1 Reactor Vessel Weld Metal

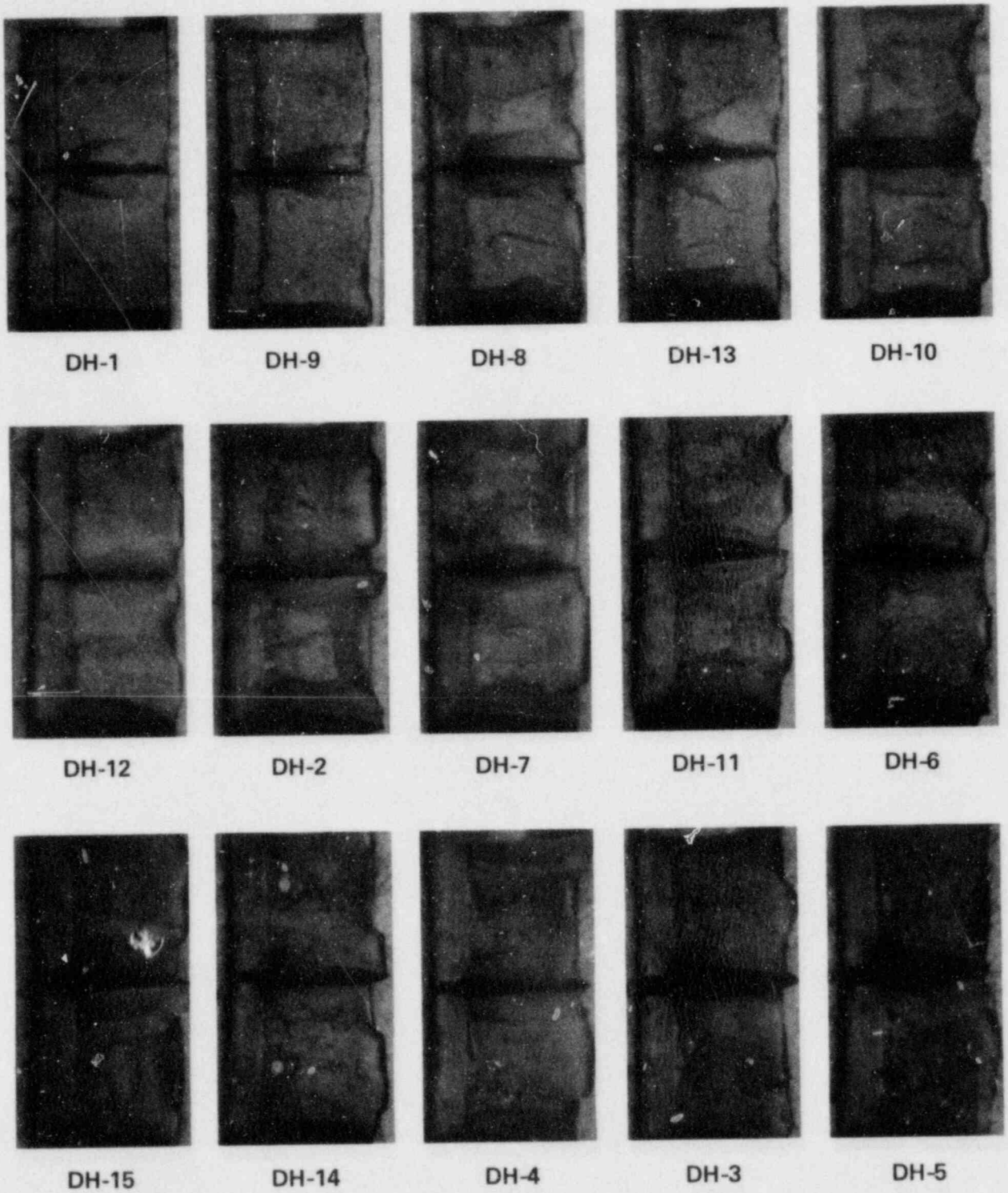

Figure 5-8. Charpy Impact Specimen Fracture Surfaces for McGuire Unit 1 Reactor Vessel Weld HAZ Metal

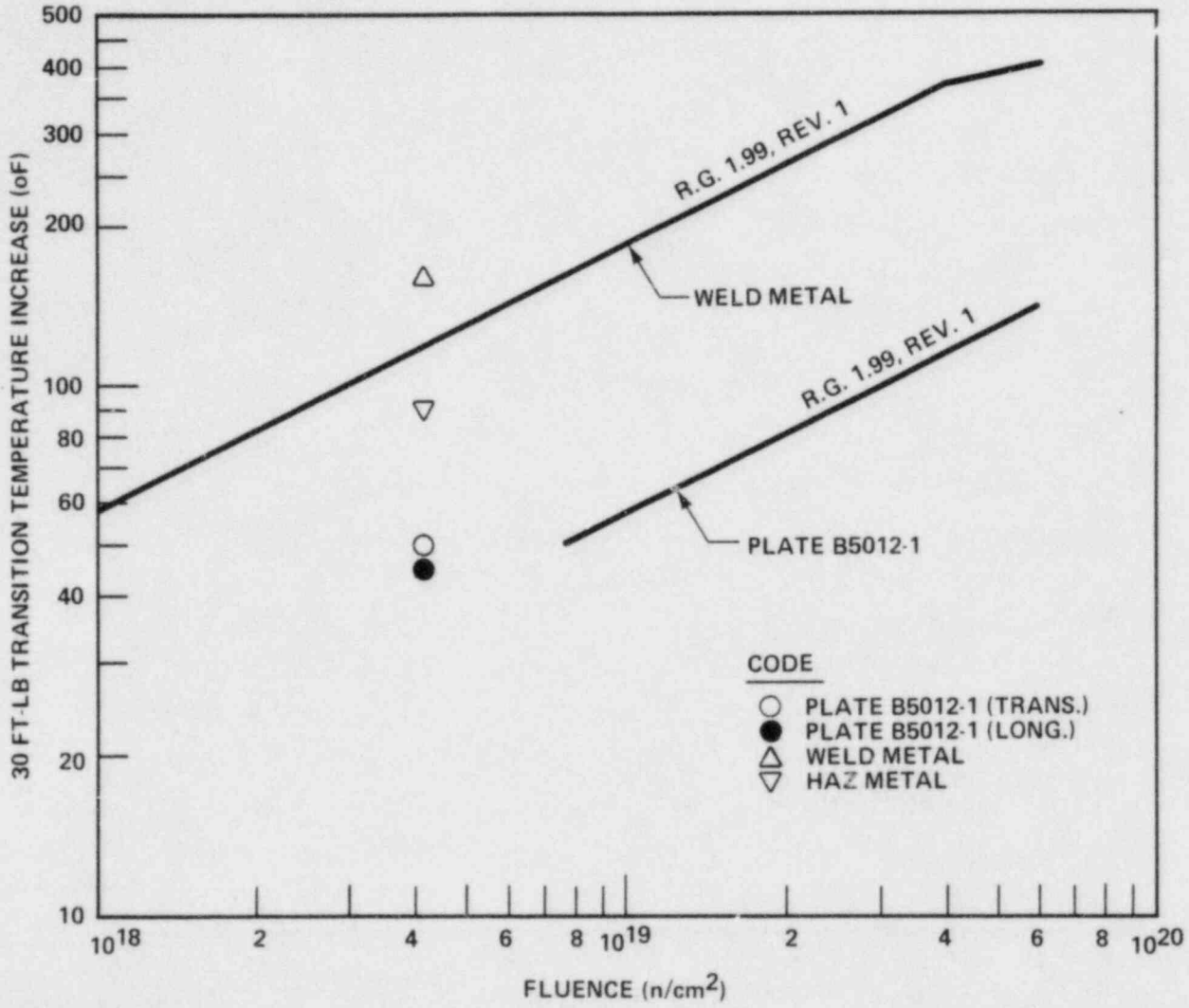

Figure 5-9. Comparison of Actual versus Predicted 30 ft-lb Transition Temperature Increases for the McGuire Unit 1 Reactor Vessel Material Based on the Prediction Methods of Regulatory Guide 1.99, Revision 1

This type of behavior is not unusual at neutron fluence levels less than 1×10^{19} n/cm^2 for relatively high copper reactor vessel weld and base materials (greater than 0.15 percent copper).

Weld HAZ specimens irradiated to 4.14×10^{18} n/cm^2 resulted in 30 ft-lb and 50 ft-lb transition temperature increases of 90°F and 95°F, respectively, as shown in figure 5-4. The upper shelf energy of the HAZ metal decreased by 10 ft-lb due to the irradiation.

The fracture appearance of each irradiated Charpy specimen from the various inadiated materials is shown in figures 5-5 through 5-8. Each of the vessel materials shows an increasing ductile or tougher appearance with increasing test temperature.

5-3. TENSION TEST RESULTS

The results of tension tests performed on material from the reactor vessel intermediate shell plate B5012-1 and weld metal irradiated to 4.14×10^{18} n/cm^2 are shown in table 5-6 and figures 5-10 through 5-12. Plate B5012-1 test results are shown in figures 5-10 and 5-11 and indicate that irradiation to 4.14×10^{18} n/cm^2 caused ~6 ksi increase in 0.2 percent yield strength and a 5 ksi increase in ultimate tensile strength. Weld metal tension test results presented in figure 5-12 show that the 0.2 percent yield strength and ultimate tensile strength increased ~ 18 ksi with irradiation. The fractured tension specimens for the plate material are shown in figures 5-13 and 5-14, while the fractured tension specimens for the weld metal are shown in figure 5-15. A typical stress strain curve for the tension tests are shown in figure 5-16.

TABLE 5-6
TENSILE PROPERTIES FOR MCGUIRE UNIT 1
REACTOR VESSEL MATERIAL IRRADIATED AT 550°F
TO 4.14 x 10^{18} n/cm^2 (E > 1.0 Mev)

Number	Material	Test Temperature (°F)	0.2% Yield Strength (ksi)	Ultimate Strength (ksi)	Fracture Load (kip)	Fracture Stress (ksi)	Fracture Strength (ksi)	Uniform Elongation (%)	Total Elongation (%)	Reduction in Area (%)
DT3	Plate B5012-1	100	71.3	91.3	3.06	173.2	62.3	11.7	23.7	64
DT1	(transverse	200	68.8	87.6	3.18	152.2	64.7	10.5	20.6	57
DT2	orientation)	550	64.7	87.6	3.22	126.5	65.6	10.5	19.0	48
DL1	Plate B5012-1	100	71.3	91.7	2.92	174.4	59.5	11.4	25.7	66
DL3	(longitudinal	200	68.8	86.6	2.75	155.6	56.0	10.5	23.4	64
DL2	orientation)	550	63.7	87.6	3.00	181.7	61.1	9.7	20.3	66
DW3	Weld metal	175	78.9	93.1	3.30	214.4	67.2	11.6	22.7	69
DW1	Weld metal	225	77.4	92.1	3.20	169.9	65.2	11.3	21.7	62
DW2	Weld metal	550	71.3	90.7	3.45	195.2	70.3	9.6	18.0	64

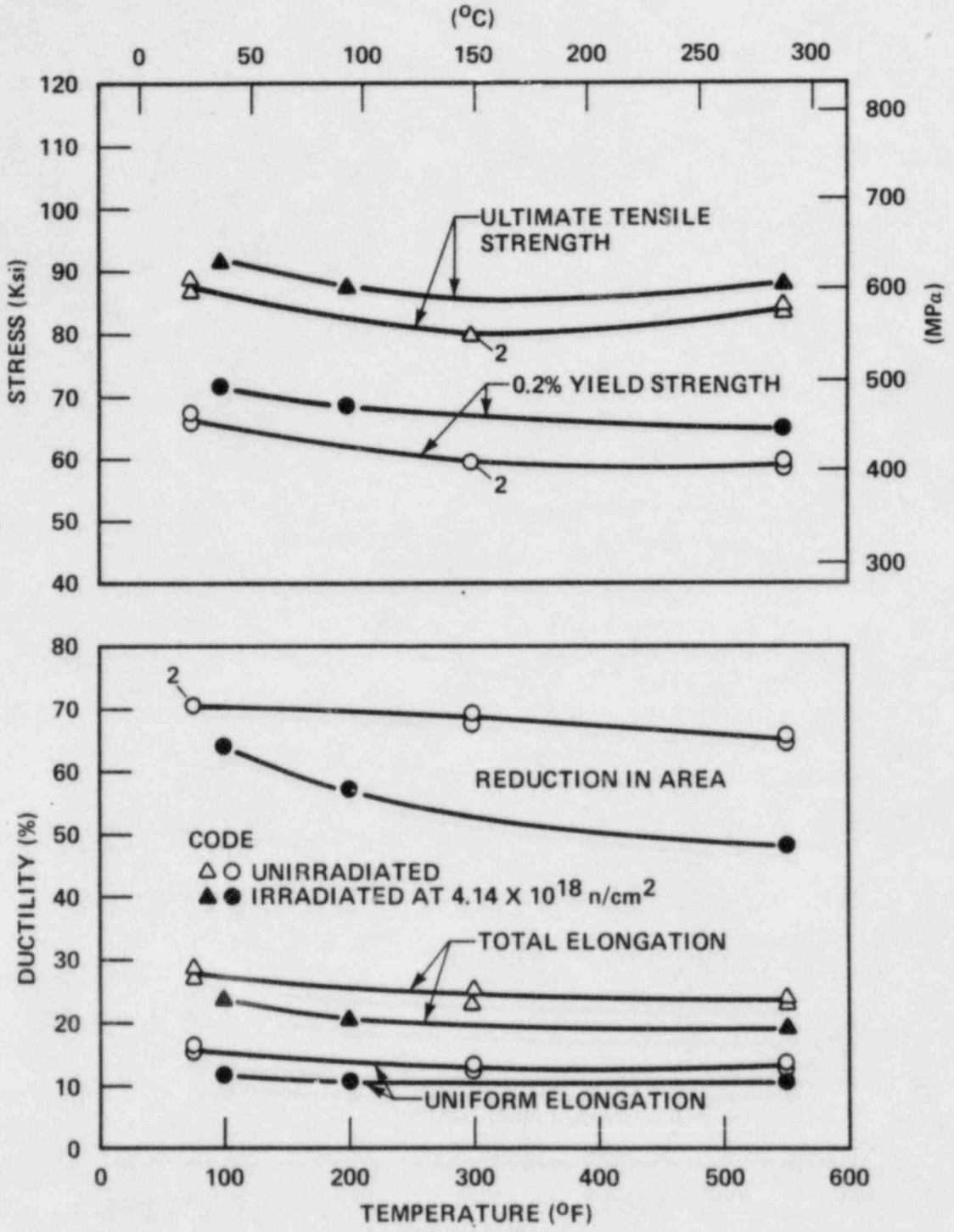

Figure 5-10. Tensile Properties for McGuire Unit 1 Reactor Vessel Shell Plate B5012-1 (Transverse Orientation)

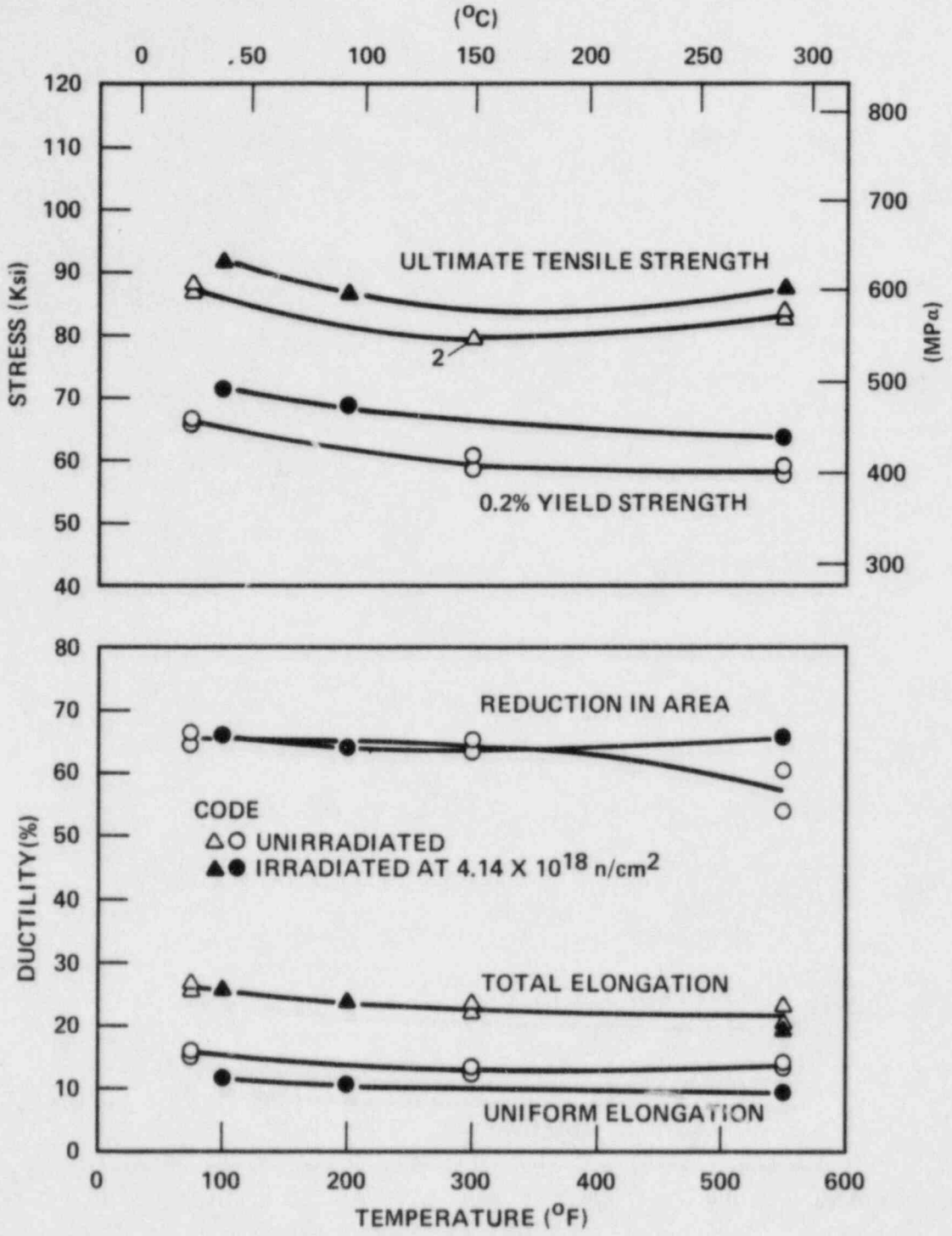

Figure 5-11. Tensile Properties for McGuire Unit 1 Reactor Vessel Shell Plate B5012-1 (Longitudinal Orientation)

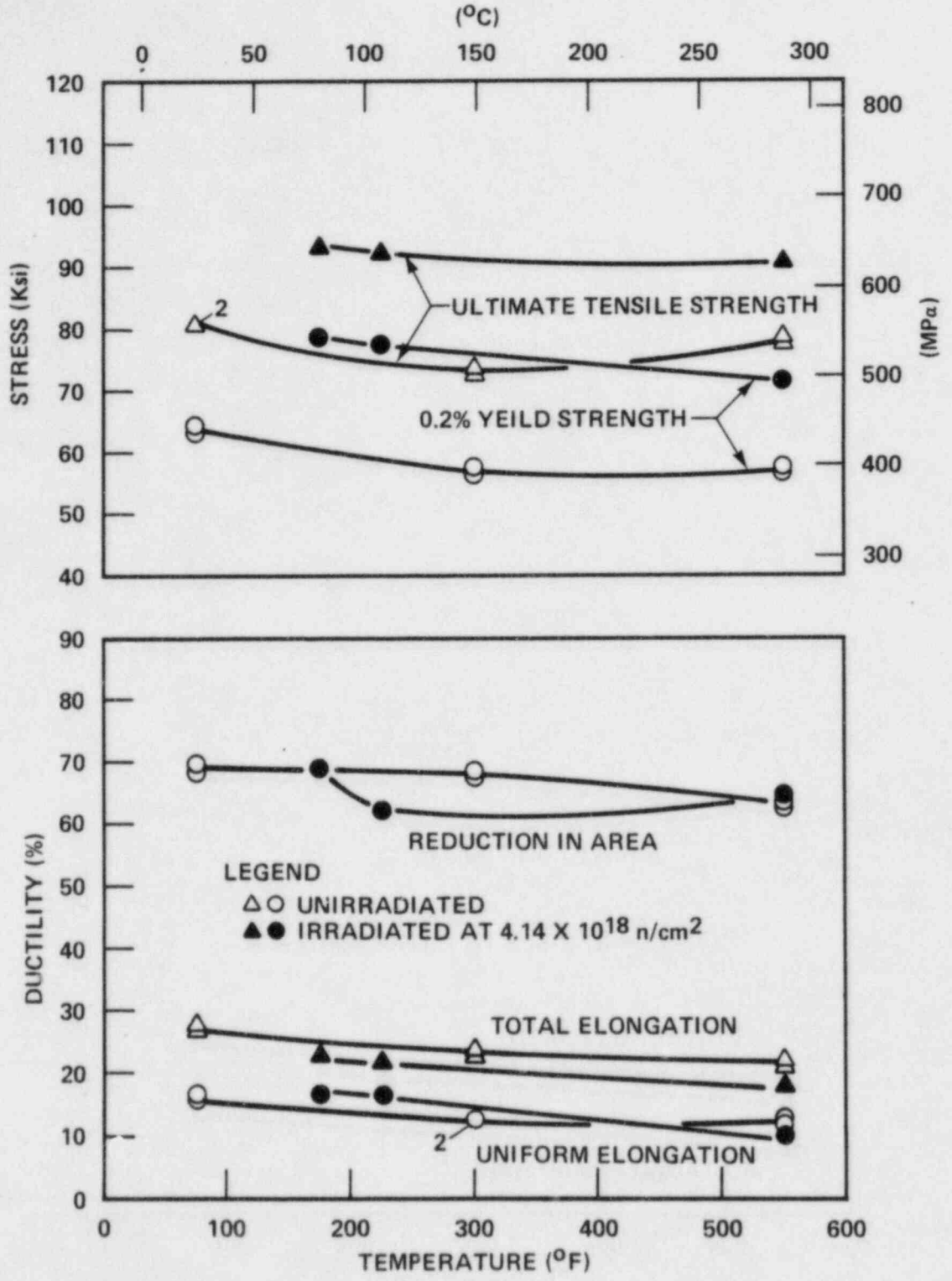

Figure 5-12. Tensile Properties for McGuire Unit 1 Reactor Vessel Weld Metal

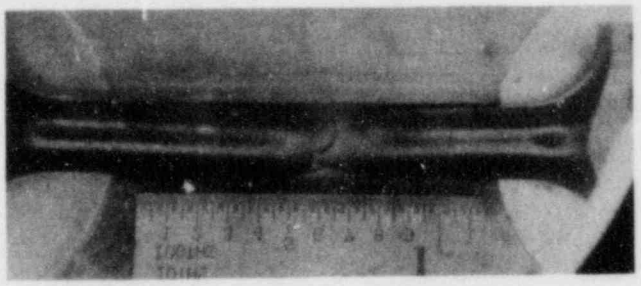

SPECIMEN DT-3 100°F

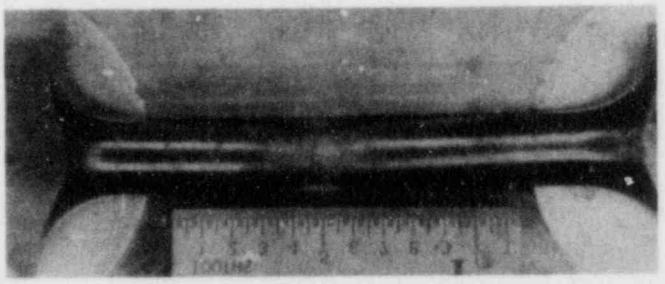

SPECIMEN DT-1 200°F

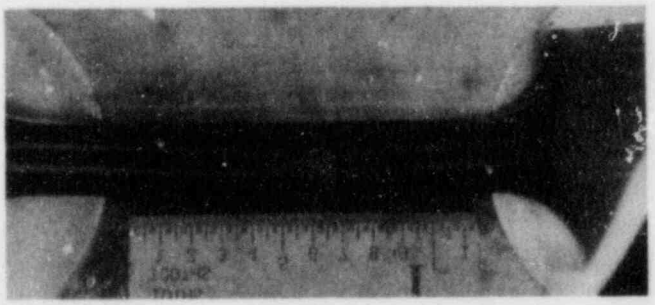

SPECIMEN DT-2 550°F

Figure 5-13. Fractured Tensile Specimens From McGuire Unit 1 Reactor Vessel Shell Plate B5012-1 (Transverse Orientation)

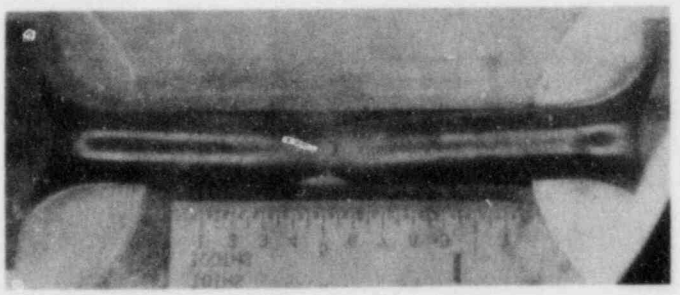

SPECIMEN DL-1 100°F

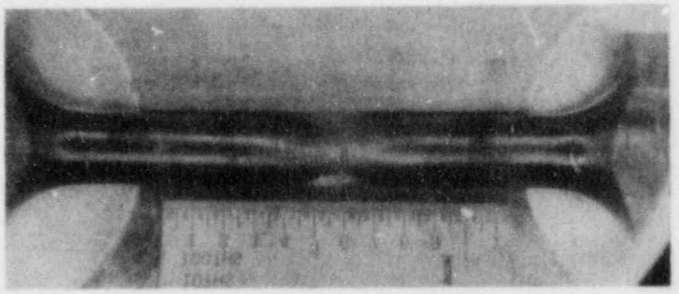

SPECIMEN DL-3 200°F

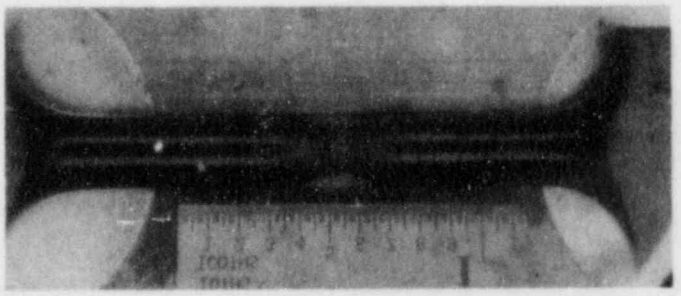

SPECIMEN DL-2 550°F

Figure 5-14. Fractured Tensile Specimens From McGuire Unit 1 Reactor Vessel Shell Plate B5012-1 (Longitudinal Orientation)

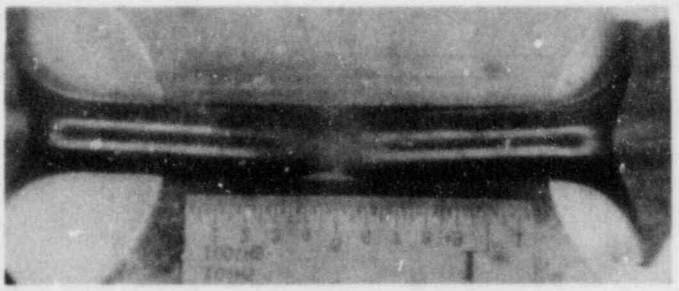

SPECIMEN DW-3 175°F

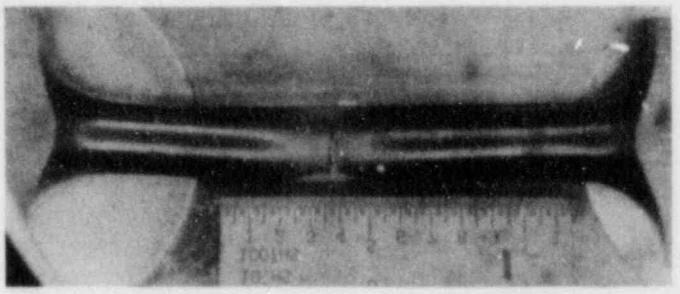

SPECIMEN DW-1 225°F

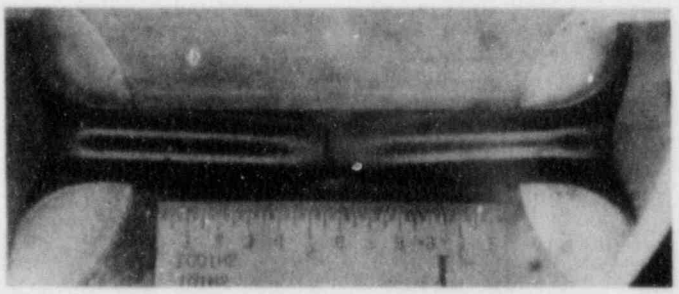

SPECIMEN DW-2 550°F

Figure 5-15. Fractured Tensile Specimens From McGuire Unit 1 Reactor Vessel Weld Metal

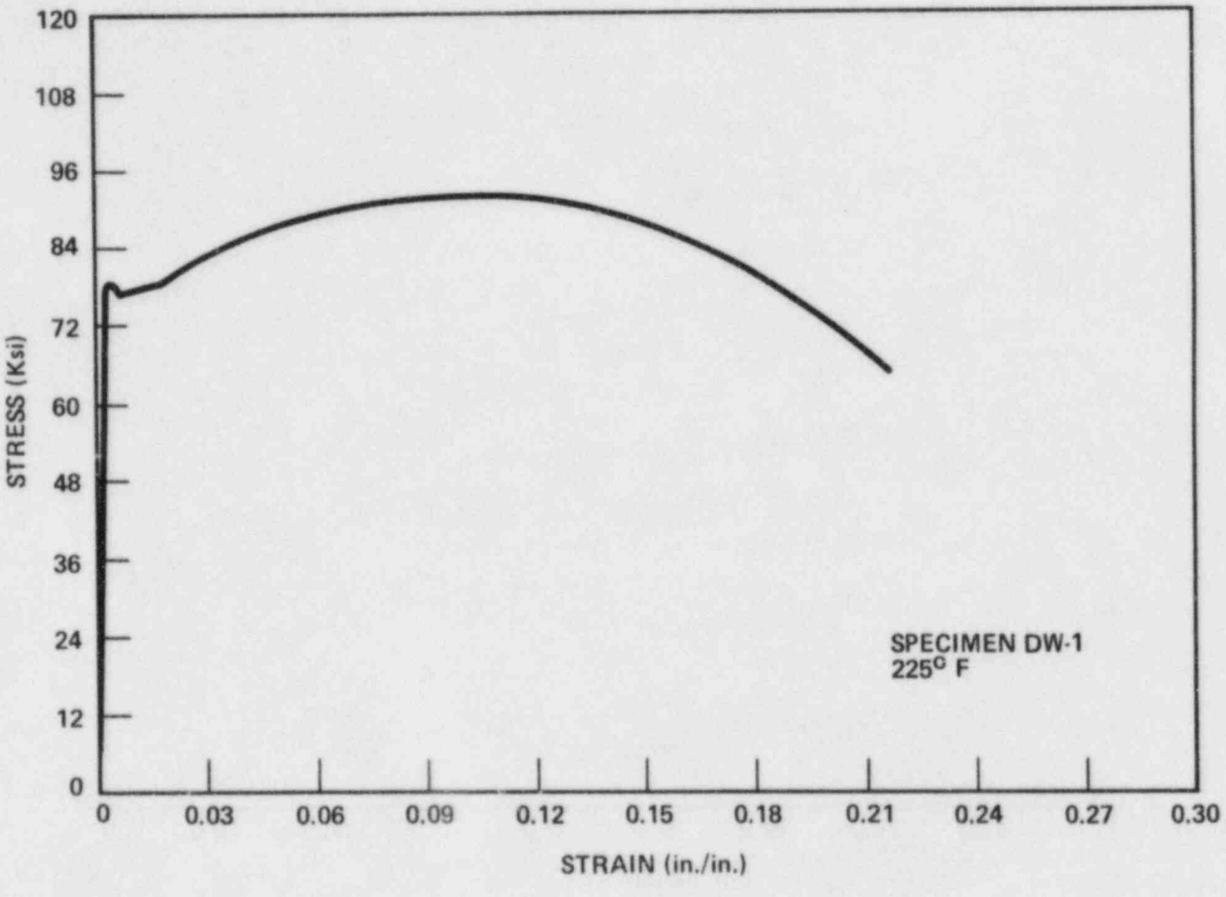

Figure 5-16. Typical Stress - Strain Curve for Tension Specimens

5-4. COMPACT TENSION TEST RESULTS

The 1/2 T compact tension fracture mechanics specimens that were contained in Capsule U have been stored at the Westinghouse Research and Development Laboratory and will be tested and reported on at a later time.

SECTION 6
RADIATION ANALYSIS AND NEUTRON DOSIMETRY

6-1. INTRODUCTION

Knowledge of the neutron environment within the pressure vessel/surveillance capsule geometry is required as an integral part of LWR pressure vessel surveillance programs for two reasons. First, in the interpretation of radiation-induced properties, changes observed in materials test specimens and the neutron environment (fluence, flux) to which the test specimens were exposed must be known. Second, in relating the changes observed in the test specimens to the present and future condition of the reactor pressure vessel, a relationship must be established between the environment at various positions within the reactor vessel and that experienced by the test specimens. The former requirement is normally met by employing a combination of rigorous analytical techniques and measurements obtained with passive neutron flux monitors contained in each of the surveillance capsules. The latter information is derived solely from analysis.

This section describes a discrete ordinates S_n transport analysis performed for the McGuire Unit 1 reactor to determine the fast neutron ($E > 1.0$ Mev) flux and fluence, as well as the neutron energy spectra within the reactor vessel and surveillance capsules. The analytical data were then used to develop lead factors for use in relating neutron exposure of the pressure vessel to that of the surveillance capsules. Based on spectrum-averaged reaction cross sections derived from this calculation, the analysis of the neutron dosimetry contained in Capsule U is presented.

6-2. DISCRETE ORDINATES ANALYSIS

A plan view of the McGuire Unit 1 reactor geometry at the core midplane is shown in figure 6-1. Since the reactor exhibits 1/8th core symmetry, only a 0- to 45-degree sector is depicted. Six irradiation capsules attached to

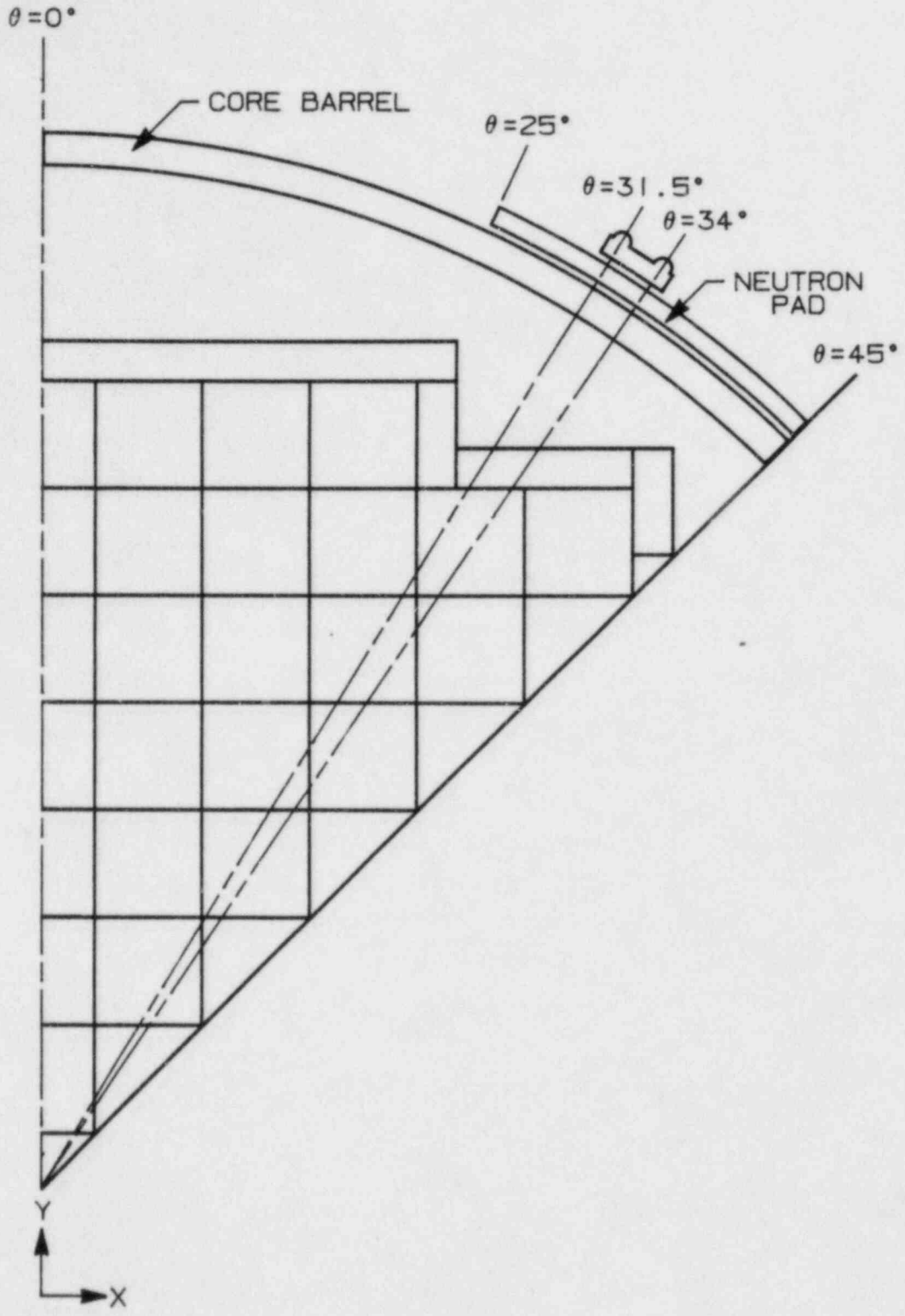

Figure 6-1. McGuire Unit 1 Reactor Geometry

the neutron pad are included in the design to constitute the reactor vessel surveillance program. Four capsules (U, W, X, Z) are located at 34° and two (V, Y) at 31.5° from the cardinal axes shown in figure 6-1.

A plan view of a double surveillance capsule attached to the neutron pad is shown in figure 6-2. The stainless steel specimen container is 1.182 inches by 1 inch and ~56 inches in height. The containers are positioned axially so that the specimens are centered on the core midplane, spanning the central 5 feet of the 12-foot high reactor core.

From a neutronic standpoint, the surveillance capsule structures are significant. In fact, as is shown later, these structures have a marked effect on the distributions of neutron flux and energy spectra in the water annulus between the neutron pad and the reactor vessel. Therefore, in order to properly ascertain the neutron environment at the test specimen locations, the capsules themselves must be included in the analytical model. Use of at least a two-dimensional computation is therefore mandatory.

In the analysis of the neutron environment within the McGuire Unit 1 reactor geometry, predictions of neutron flux magnitude and energy spectra were made with the DOT[4] two-dimensional discrete ordinates code. The radial and azimuthal distributions were obtained from an R,θ computation wherein the geometry shown in figures 6-1 and 6-2 was described in the analytical model. In addition to the R,θ computation, a second calculation in R,Z geometry was also carried out to obtain relative axial variations of neutron flux throughout the geometry of interest. In the R,Z analysis, the reactor core was treated as an equivalent volume cylinder and, of course, the surveillance capsules were not included in the model.

Both the R,θ and R,Z analyses employed 47 neutron energy groups and a P_3 expansion of the scattering cross sections. The cross sections used in the analyses were obtained from the SAILOR cross section library[5] which was developed specifically for light water reactor applications. The neutron energy group structure used in the analysis is listed in table 6-1.

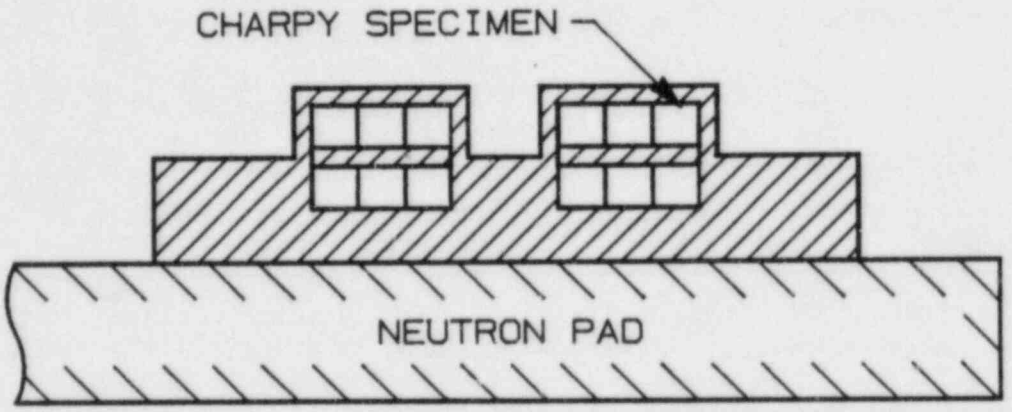

Figure 6-2. Plan View of a Reactor Vessel Surveillance Capsule

TABLE 6-1

47 GROUP ENERGY STRUCTURE

Group	Lower Energy (Mev)	Group	Lower Energy (Mev)
1	14.19[a]	25	0.183
2	12.21	26	0.111
3	10.00	27	0.0674
4	8.61	28	0.0409
5	7.41	29	0.0318
6	6.07	30	0.0261
7	4.97	31	0.0242
8	3.68	32	0.0219
9	3.01	33	0.0150
10	2.73	34	7.10×10^{-3}
11	2.47	35	3.36×10^{-3}
12	2.37	36	1.59×10^{-3}
13	2.35	37	4.54×10^{-4}
14	2.23	38	2.14×10^{-4}
15	1.92	39	1.01×10^{-4}
16	1.65	40	3.73×10^{-5}
17	1.35	41	1.07×10^{-5}
18	1.00	42	5.04×10^{-6}
19	0.821	43	1.86×10^{-6}
20	0.743	44	8.76×10^{-7}
21	0.608	45	4.14×10^{-7}
22	0.498	46	1.00×10^{-7}
23	0.369	47	0.00
24	0.298	--	--

a. The upper energy of group 1 is 17.33 Mev

A key input parameter in the analysis of the integrated fast neutron exposure of the reactor vessel is the core power distribution. For this analysis, power distributions representative of time-averaged conditions derived from statistical studies of long-term operation of Westinghouse four-loop plants were employed. These input distributions include rod-by-rod spatial variations for all peripheral fuel assemblies.

It should be noted that this generic design basis power distribution is intended to provide a vehicle for long-term End-Of-Life (EOL) prejection of vessel exposure. Since plant-specific power distributions reflect only past operation, their use for projection into the future may not be justified; the use of generic data which reflects long-term operation of similar reactor cores may provide a more suitable approach.

Benchmark testing of these generic power distributions and the SAILOR cross sections against surveillance capsule data obtained from two-loop and four-loop Westinghouse plants indicate that this analytical approach yields conservative results, with calculations exceeding measurements from 10 to 25 percent[6].

One further point of interest regarding these analyses is that the design basis assumes an out-in fuel loading pattern (fresh fuel on the periphery). Future commitment to low-leakage loading patterns could significantly reduce the calculated neutron flux levels presented in section 6-4. In addition, capsule lead factors could be changed influencing the withdrawal schedule of the remaining surveillance capsules.

Having the results of the R,θ and R,Z calculations, three-dimensional variations of neutron flux may be approximated by assuming that the following relation holds for the applicable regions of the reactor.

$$\phi(R,Z,\theta,E_g) = \phi(R,\theta,E_g) \times F(Z,E_g) \qquad (6\text{-}1)$$

where

$\phi(R,Z,\theta,E_g)$ = neutron flux at point R,Z,θ within energy group g

$\phi(R,\theta,E_g)$ = neutron flux at point R,θ within energy group g obtained from the R,θ calculation

$F(Z,E_g)$ = relative axial distribution of neutron flux within energy group g obtained from the R,Z calculation

6-3. NEUTRON DOSIMETRY

The passive neutron flux monitors included in the McGuire Unit 1 surveillance program are listed in table 6-2. The first five reactions in table 6-2 are used as fast neutron monitors to relate neutron fluence (E > 1.0 Mev) to measured material property changes. To properly account for burnout of the product isotope generated by fast neutron reactions, it is necessary to also determine the magnitude of the thermal neutron flux at the monitor location. Therefore, bare and cadmium-covered cobalt-aluminum monitors were also included.

TABLE 6-2

NUCLEAR CONSTANTS FOR NEUTRON FLUX MONITORS CONTAINED IN THE McGUIRE UNIT 1 SURVEILLANCE CAPSULES

Monitor Material	Reaction of Interest	Target Weignt Fraction	Fission Product Half-Life	Yield (%)
Copper	Cu^{63} (n,α) Co^{60}	0.6917	5.27 years	--
Iron	Fe^{54} (n,p) Mn^{54}	0.0585	314 days	--
Nickel	Ni^{58} (n,p) Co^{58}	0.6777	71.4 days	--
Uranium-238[a]	U^{238} (n,f) Cs^{137}	1.0	30.2 years	6.3
Neptunium-237[a]	Np^{237} (n,f) Cs^{137}	1.0	30.2 years	6.5
Cobalt-aluminum[a]	Co^{59} (n,γ) Co^{60}	0.0015	5.27 years	--
Cobalt-aluminum	Co^{59} (n,γ) Co^{60}	0.0015	5.27 years	--

a. Denotes that monitor is cadmium-shielded

The relative locations of the various monitors within the surveillance capsule are shown in figure 4-2. The iron, nickel, copper, and cobalt-aluminum monitors, in wire form, are placed in holes drilled in spacers at several axial levels within the capsules. The cadmium-shielded neptunium and uranium fission monitors are accommodated within the dosimeter block located near the center of the capsule.

The use of passive monitors such as those listed in table 6-2 does not yield a direct measure of the energy-dependent flux level at the point of interest. Rather, the activation or fission process is a measure of the integrated effect that the time- and energy-dependent neutron flux has on the target material over the course of the irradiation period. An accurate assessment of the average neutron flux level incident on the various monitors may be derived from the activation measurements only if the irradiation parameters are well known. In particular, the following variables are of interest.

- The operating history of the reactor
- The energy response of the monitor
- The neutron energy spectrum at the monitor location
- The physical characteristics of the monitor

The analysis of the passive monitors and subsequent derivation of the average neutron flux requires completion of two operations. First, the disintegration rate of product isotope per unit mass of monitor must be determined. Second, in order to define a suitable spectrum-averaged reaction cross section, the neutron energy spectrum at the monitor location must be calculated.

The specific activity of each of the monitors is determined using established ASTM procedures [7,8,9,10,11]. Following sample preparation, the activity of each monitor is determined by means of a lithium-drifted germanium, Ge(Li), gamma spectrometer. The overall standard deviation of the measured data is a function of the precision of sample weighing, the uncertainty in counting, and the acceptable error in detector calibration. For the samples removed from

McGuire Unit 1, the overall 2σ deviation in the measured data is determined to be ±10 percent. The neutron energy spectra are determined analytically using the method described in section 6-1.

Having the measured activity of the monitors and the neutron energy spectra at the locations of interest, the calculation of the neutron flux proceeds as follows. The reaction product activity in the monitor is expressed as follows.

$$R = \frac{N_o}{A} f_i y \int_E \sigma(E)\phi(E)dE \sum_{j=1}^{n} \frac{P_j}{P_{max}} (1-e^{-\lambda t_j}) e^{-\lambda t_d} \qquad (6\text{-}2)$$

where

R	=	induced product activity
N_o	=	Avogadro's number
A	=	atomic weight of the target isotope
f_i	=	weight fraction of the target isotope in the target material
Y	=	number of product atoms produced per reaction
$\sigma(E)$	=	energy dependent reaction cross section
$\phi(E)$	=	energy dependent neutron flux at the monitor location with the reactor at full power
P_j	=	average core power level during irradiation period j
P_{max}	=	maximum or reference core power level
λ	=	decay constant of the product isotope
t_j	=	length of irradiation period j
t_d	=	decay time following irradiation period j

Because neutron flux distributions are calculated using multigroup transport methods and, further, because the prime interest is in the fast neutron flux above 1.0 Mev, spectrum-averaged reaction cross sections are defined so that the integral term in equation 6-2 is replaced by the following relationship.

$$\int_E \sigma(E)\phi(E)dE = \bar{\sigma}\,\phi \quad (E > 1.0 \text{ Mev})$$

where

$$\bar{\sigma} = \frac{\int_0^{\infty} \sigma(E)\phi(E)dE}{\int_{1.0\text{ Mev}}^{\infty} \phi(E)dE} = \frac{\sum_{g=1}^{N} \sigma_g \phi_g}{\sum_{g=g_{1.0\text{ Mev}}}^{N} \phi_g}$$

Therefore, equation 6-2 is rewritten

$$R = \frac{N_o}{A} f_i \, Y \, \bar{\sigma} \, \phi \, (E > 1.0 \text{ Mev}) \sum_{j=1}^{N} \frac{P_j}{P_{max}} (1-e^{-\lambda t_j}) \, e^{-\lambda t_d}$$

or, solving for the neutron flux,

$$\phi(E > 1.0 \text{ Mev}) = \frac{R}{\frac{N_o}{A} f_i \, Y \, \bar{\sigma} \sum_{j=1}^{n} \frac{P_j}{P_{max}} (1-e^{-\lambda t_j}) \, e^{-\lambda t_d}} \qquad (6\text{-}3)$$

The total fluence above 1.0 Mev is then given by

$$\Phi(E > 1.0 \text{ Mev}) = \phi(E > 1.0 \text{ Mev}) \sum_{j=1}^{n} \frac{P_j}{P_{max}} t_j \qquad (6\text{-}4)$$

where

$\sum_{j=1}^{n} \frac{P_j}{P_{max}} t_j$ = total effective full power seconds of reactor operation up to the time of capsule removal

An assessment of the thermal neutron flux levels within the surveillance capsules is obtained from the bare and cadmium-covered Co^{59} (n,γ) Co^{60} data by means of cadmium ratios and the use of a 37-barn, 2,200 m/sec cross section.

$$\phi_{Th} = \frac{R_{bare}\left[\frac{D-1}{D}\right]}{\frac{N_o f_i}{A} Y\sigma \sum_{j=1}^{n} \frac{P_j}{P_{max}} (1-e^{-\lambda t_j}) \, e^{-\lambda t_d}} \qquad (6\text{-}5)$$

where

$D = R_{bare}/R_{Cd\ covered}$

6-4. TRANSPORT ANALYSIS RESULTS

Results of the S_n transport calculations for the McGuire Unit 1 reactor are summarized in figures 6-3 through 6-6 and in tables 6-3 through 6-5. In figure 6-3, the calculated maximum neutron flux levels at the surveillance capsule centerline, pressure vessel inner radius, 1/4-thickness location, and 3/4-thickness location are presented as a function of azimuthal angle. The influence of the surveillance capsules on the fast neutron flux distribution is clearly evident. In figure 6-4, the radial distribution of maximum fast neutron flux ($E > 1.0$ Mev) through the thickness of the reactor pressure vessel is shown. The relative axial variation of neutron flux within the vessel is given in figure 6-5. Absolute axial variations of fast neutron flux may be obtained by multiplying the levels given in figure 6-3 or 6-4 by the appropriate values from figure 6-5.

In figure 6-6, the radial variations of fast neutron flux within the surveillance capsules are presented. These data, in conjunction with the maximum vessel flux, are used to develop lead factors for each of the capsules. Here the lead factor is defined as the ratio of the fast neutron flux ($E > 1.0$ Mev) at the dosimeter block location (capsule center) to the maximum fast neutron flux at the pressure vessel inner radius. The updated lead factors for the McGuire Unit 1 surveillance capsules are listed in table 6-3. The neutron flux monitors contained within the surveillance capsule are all located at the same radial location, the capsule center. Had they been located at different radial locations within the capsules it would have been necessary to adjust the disintegration rates for the gradients that exist within the capsules. In the present analysis, the point of comparison for all reaction rates is, of course, the capsule center.

In order to derive neutron flux and fluence levels from the measured disintegration rates, suitable spectrum-averaged reaction cross sections are required. The neutron energy spectrum calculated to exist at the center of the McGuire Unit 1 surveillance Capsule U is listed in table 6-4. The associated spectrum-averaged cross sections for each of the fast neutron reactions are given in table 6-5.

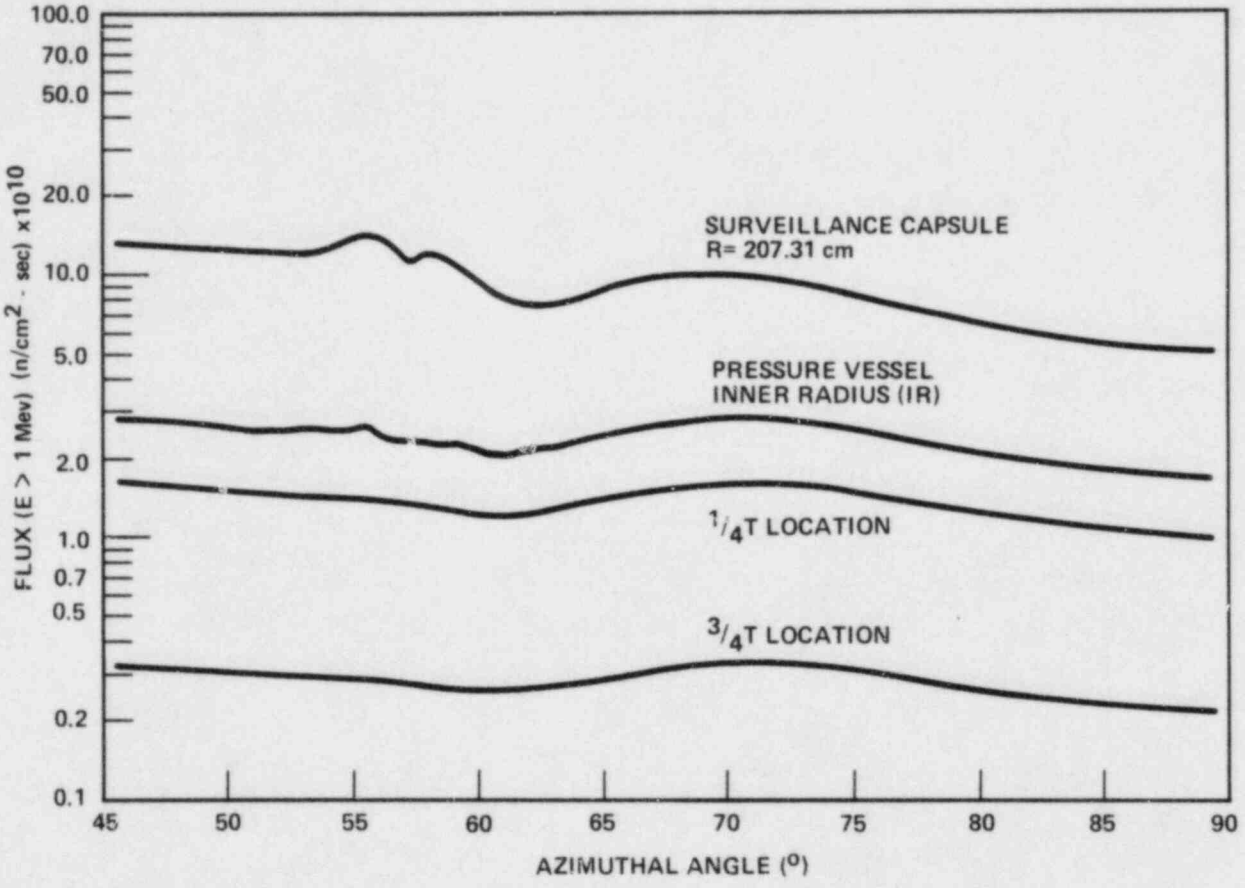

Figure 6-3. Calculated Azimuthal Distribution of Maximum Fast Neutron Flux (E > 1.0 Mev) Within the Pressure Vessel - Surveillance Capsule Geometry

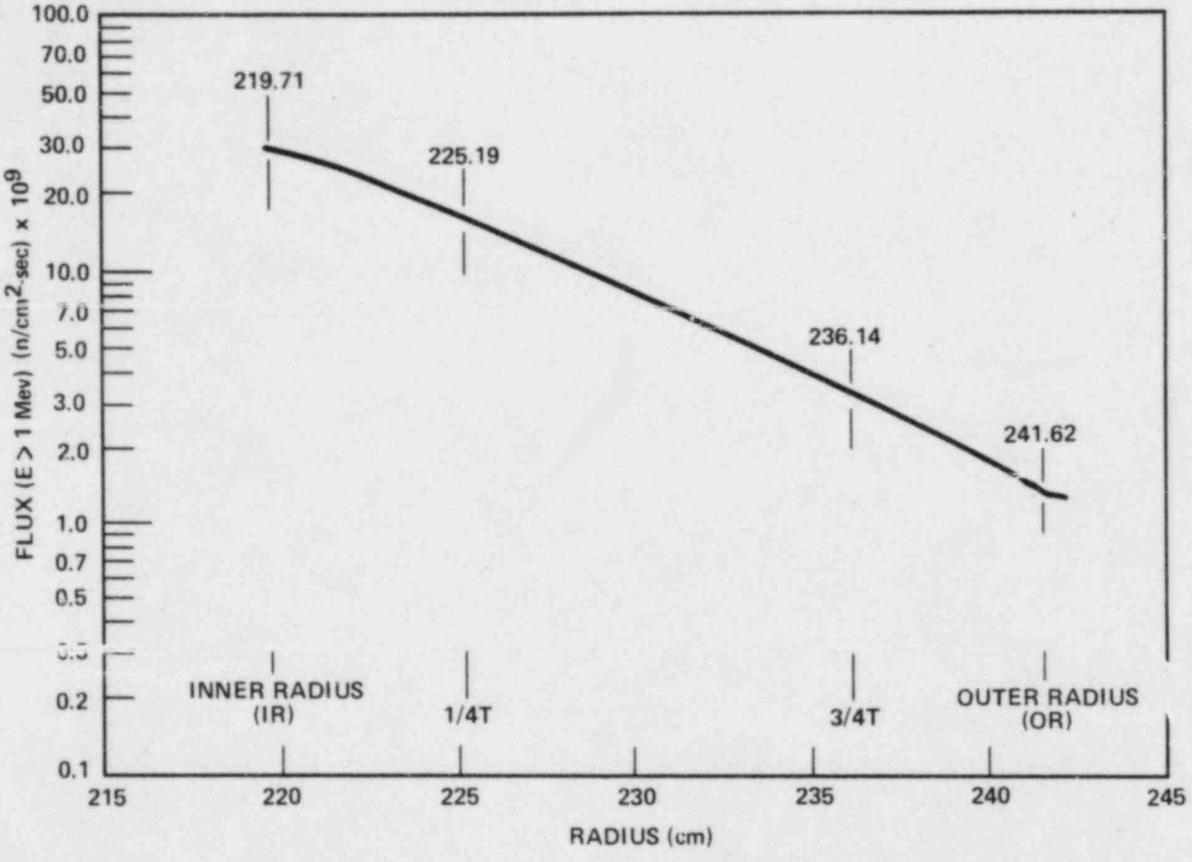

Figure 6-4. Calculated Radial Distribution of Maximum Fast Neutron Flux (E >1.0 Mev) Within the Pressure Vessel

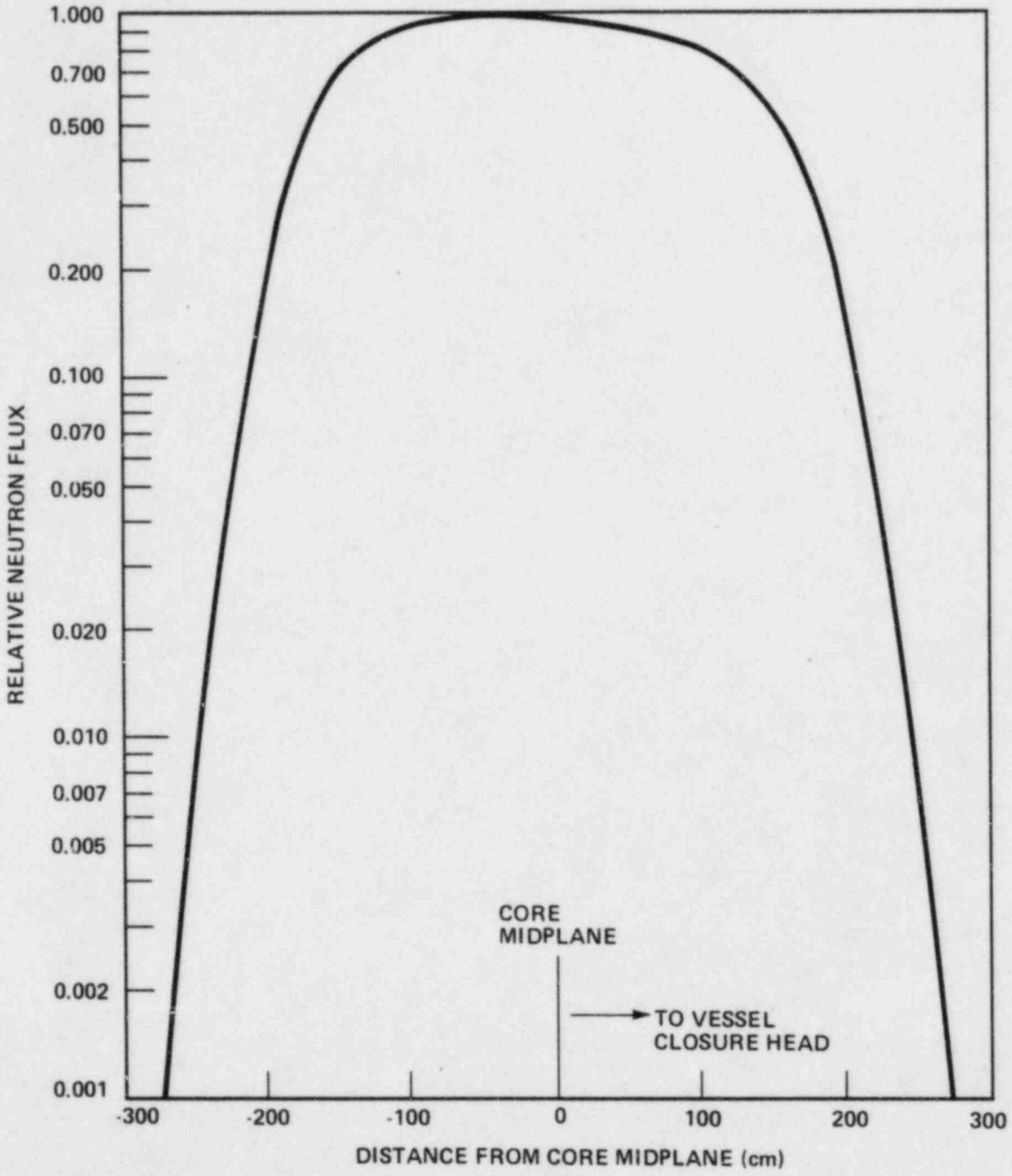

Figure 6-5. Relative Axial Variation of Fast Neutron Flux (E >1.0 Mev) Within the Pressure Vessel

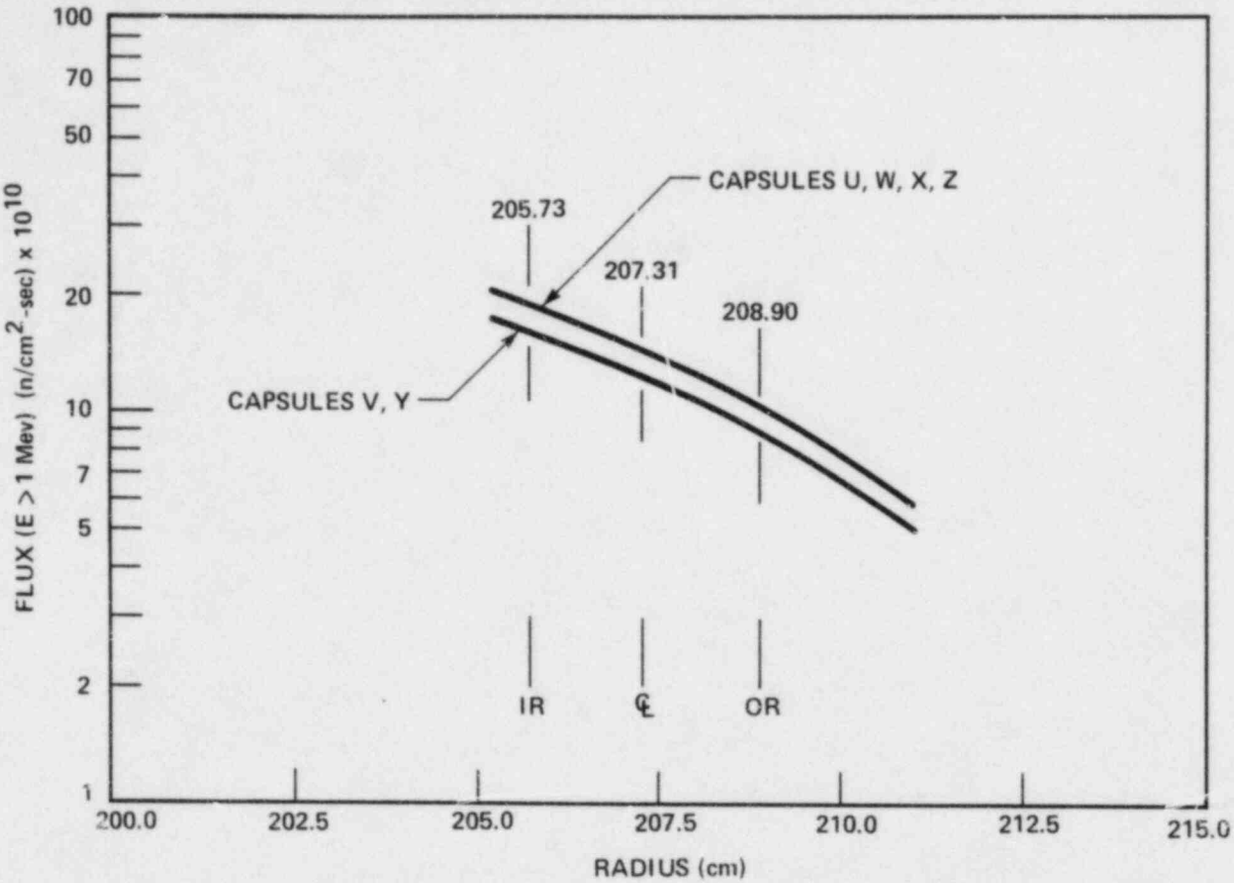

Figure 6-6. Calculated Radial Distribution of Maximum Fast Neutron Flux (E > 1.0 Mev) Within the Surveillance Capsules

TABLE 6-3

CALCULATED FAST NEUTRON FLUX (E > 1.0 Mev) AND LEAD FACTOR FOR McGUIRE UNIT 1 SURVEILLANCE CAPSULES

Capsule	Azimuthal Location (°)	ϕ(E > 1.0 Mev) (n/cm^2 - sec)	Lead Factor
U	56°	1.4231×10^{11}	4.76
W	124°	1.4231×10^{11}	4.76
X	236°	1.4231×10^{11}	4.76
Z	304°	1.4231×10^{11}	4.76
V	58.5°	1.21536×10^{11}	4.06
Y	238.5°	1.21536×10^{11}	4.06

TABLE 6-4

CALCULATED NEUTRON ENERGY SPECTRA AT THE CENTER OF THE McGUIRE UNIT 1 SURVEILLANCE CAPSULE U

Group No.	ϕ (n/cm^2-sec)	Group No.	ϕ (n/cm^2-sec)
1	2.33290×10^{7}	25	8.24716×10^{10}
2	8.56092×10^{7}	26	8.59363×10^{10}
3	2.98276×10^{8}	27	6.91292×10^{10}
4	5.45563×10^{8}	28	4.84202×10^{10}
5	9.11017×10^{8}	29	1.44982×10^{10}
6	2.02395×10^{9}	30	7.80675×10^{9}
7	2.81044×10^{9}	31	2.13876×10^{10}
8	5.80793×10^{9}	32	1.38042×10^{10}
9	5.41035×10^{9}	33	2.43642×10^{10}
10	4.54219×10^{9}	34	3.56461×10^{10}
11	5.47463×10^{9}	35	6.05357×10^{10}
12	2.74190×10^{9}	36	5.44679×10^{10}
13	8.41871×10^{8}	37	7.61645×10^{10}
14	4.24241×10^{9}	38	4.13856×10^{10}
15	1.14137×10^{10}	39	4.59692×10^{10}
16	1.55890×10^{10}	40	6.22153×10^{10}
17	2.43599×10^{10}	41	7.34671×10^{10}
18	5.51878×10^{10}	42	4.06677×10^{10}
19	4.25406×10^{10}	43	4.63747×10^{10}
20	2.01268×10^{10}	44	2.87056×10^{10}
21	7.41069×10^{10}	45	2.22168×10^{10}
22	5.81217×10^{10}	46	3.11690×10^{10}
23	7.26368×10^{10}	47	3.97555×10^{10}
24	7.08945×10^{10}	--	--

TABLE 6-5

SPECTRUM-AVERAGED REACTION CROSS SECTIONS AT THE CENTER OF McGUIRE UNIT 1 SURVEILLANCE CAPSULE U (θ=56°)

Reaction	$\bar{\sigma}$ [a] (barns)
Fe^{54} (n,p) Mn^{54}	0.0559
Cu^{63} (n,α) Co^{60}	0.000479
Ni^{58} (n,p) Co^{58}	0.0779
Np^{237} (n,f) Cs^{137}	3.338
U^{238}(n,f) Cs^{137}	0.313
Co^{59} (n,γ) Co^{60}	23

---

a. $$\bar{\sigma} = \frac{\int_0^\infty \sigma(E)\phi(E)dE}{\int_{1\ Mev}^\infty \phi(E)dE}$$

6-5. DOSIMETRY RESULTS

The irradiation history of the McGuire Unit 1 reactor up to the time of removal of Capsule U is listed in table 6-6. Comparisons of measured and calculated saturated activity of the flux monitors contained in Capsule U based on the irradiation history shown in table 6-6 are listed in table 6-7. The data are presented as measured at the capsule center.

The fast neutron (E > 1.0 Mev) flux and fluence levels derived for Capsule U are presented in table 6-8. The thermal neutron flux obtained from the cobalt-aluminum monitors is summarized in table 6-9. Due to the relatively low thermal neutron flux at the capsule location, no burnup correction was made to any of the measured activities. The maximum error introduced by this assumption is estimated to be < 1 percent for the Ni^{58} $(n,p)Co^{58}$ reaction and even less significant for all of the other fast neutron reactions.

An examination of table 6-8 shows that the fast neutron flux (E > 1.0 Mev) derived from the five threshold reactions ranges from 1.12×10^{11} to 1.35×10^{11} n/cm^2-sec, a total span of less than 21 percent. It may also be noted that the calculated flux value of 1.42×10^{11} n/cm^2-sec exceeds all of the measured values, with calculation to experimental ratios ranging from 1.05 to 1.27.

Comparisons of measured and calculated current fast neutron exposures for Capsule U and the Inner Radius (IR) of the pressure vessel are presented in table 6-10. Calculated current and EOL vessel exposures are presented in table 6-11, for vessel inner radius, 1/4 thickness and 3/4 thickness. The measured value is given based on the average of all five threshold reactions. Based on the data given in table 6-10, the best estimate exposure of Capsule U is as below.

$$\phi_T = 4.13 \times 10^{18} \text{ n/cm}^2 \text{ (E > 1.0 Mev)}$$

TABLE 6-6

IRRADIATION HISTORY OF McGUIRE UNIT 1

SURVEILLANCE CAPSULE U

Month	Year	Pj (mw)	Pmax (mw)	P_j/P_{max}	Irradiation Time[a] (day)	Decay Time[b] (day)
10	1981	296	3565	0.083	31	1077
11	1981	1089	3565	0.306	30	1047
12	1981	112	3565	0.031	31	1016
1	1982	1771	3565	0.497	31	985
2	1982	1443	3565	0.405	28	957
3	1982	694	3565	0.195	31	926
4	1982	1660	3565	0.466	30	896
5	1982	2000	3565	0.561	31	865
6	1982	1804	3565	0.506	30	835
7	1982	755	3565	0.212	31	804
8	1982	1981	3565	0.556	31	773
9	1982	2040	3565	0.572	30	743
10	1982	1814	3565	0.509	31	712
11	1982	735	3565	0.206	30	682
12	1982	1702	3565	0.477	31	651
1	1983	1154	3565	0.324	31	620
2	1983	0	3565	0.000	28	592
3	1983	0	3565	0.000	31	561
4	1983	0	3565	0.000	30	531
5	1983	233	3565	0.065	31	500
6	1983	2783	3565	0.781	30	470
7	1983	2718	3565	0.762	31	439
8	1983	1547	3565	0.434	31	408
9	1983	3225	3565	0.905	30	378
10	1983	2682	3565	0.752	31	347
11	1983	2619	3565	0.735	30	317
12	1983	2804	3565	0.787	31	286
1	1984	3146	3565	0.882	31	255
2	1984	2692	3565	0.755	29	226
3	1984	0	3565	0.000	1	225

a. Total irradiation time = 3.36×10^7 Effective Full Power Seconds (EFPS)
b. Decay time is referenced to 10/12/84

TABLE 6-7
COMPARISON OF MEASURED AND CALCULATED FAST NEUTRON FLUX
MONITOR SATURATED ACTIVITIES FOR CAPSULE U

Reaction and Axial Position	Radial Location (cm)	Saturated Activity (dps/gm) Actual for Capsule U	Saturated Activity (dps/gm) Calculated for Capsule U
Fe^{54} (n,p) Mn^{54}			
Top	207.31	3.97×10^6	
Middle	207.31	4.10×10^6	
Bottom	207.31	4.16×10^6	
AVERAGE		4.08×10^6	5.19×10^6
Cu^{63} (n,α) Co^{60}			
Top	207.31	3.96×10^5	
Middle	207.31	4.16×10^5	
Bottom	207.31	3.98×10^5	
AVERAGE		4.03×10^5	4.50×10^5
Ni^{58} (n,p) Co^{58}			
Top	207.31	6.04×10^7	
Middle	207.31	6.30×10^7	
Bottom	207.31	6.52×10^7	
AVERAGE		6.29×10^7	7.81×10^7
Np^{237} (n,f) Cs^{137}			
Middle	207.31	7.01×10^7	7.80×10^7
U^{238} (n,f) Cs^{137}			
Middle	207.31	7.65×10^6	7.10×10^6

TABLE 6-8
RESULTS OF FAST NEUTRON DOSIMETRY FOR CAPSULE U

Reaction	Adjusted Saturated Activity (dps/gm)		ϕ (E > 1.0 Mev) (n/cm^2-sec)		Φ (E > 1.0 Mev) (n/cm^2)	
	Measured	Calculated	Measured	Calculated	Measured	Calculated
$Fe^{54}(n,p)Mn^{54}$	4.08×10^6	5.19×10^6	1.12×10^{11}	1.42×10^{11}	3.75×10^{18}	4.78×10^{18}
$Cu^{63}(n,\alpha)Co^{60}$	4.03×10^5	4.50×10^5	1.27×10^{11}	1.42×10^{11}	4.27×10^{18}	4.78×10^{18}
$Ni^{58}(n,p)Co^{58}$	6.29×10^7	7.81×10^7	1.15×10^{11}	1.42×10^{11}	3.85×10^{18}	4.78×10^{18}
$Np^{237}(n,f)Cs^{137}$	7.01×10^7	7.80×10^7	1.27×10^{11}	1.42×10^{11}	4.27×10^{18}	4.78×10^{18}
$U^{238}(n,f)Cs^{137}$	6.73×10^{6}[a]	7.10×10^6	1.35×10^{11}[a]	1.42×10^{11}	4.52×10^{18}[a]	4.78×10^{18}

a. U^{238} adjusted saturated activity has been multiplied by 0.88 to correct for 350 ppm U^{235} impurity

TABLE 6-9

RESULTS OF THERMAL NEUTRON DOSIMETRY FOR CAPSULE U

Axial Location	Saturated Activity (dps/gm) Bare	Cd-covered	ϕ_{Th} (n/cm^2-sec)
Top	1.13×10^8	5.65×10^7	1.59×10^{11}
Middle	9.45×10^7	5.59×10^7	1.09×10^{11}
Bottom	9.37×10^7	5.68×10^7	1.05×10^{11}
AVERAGE	1.00×10^8	5.64×10^7	1.24×10^{11}

TABLE 6-10

SUMMARY OF FAST NEUTRON DOSIMETRY RESULTS FOR CAPSULE U

Basis	Irradiation Time (EFPS)	ϕ(E>1.0 Mev) (n/cm^2-sec)	Φ(E>1.0 Mev) (n/cm^2)	Lead Factor	Vessel Fluence (n/cm^2)	Calculated Vessel Fluence (n/cm^2)
$Fe^{54}(n,p)Mn^{54}$	3.36×10^7	1.12×10^{11}	3.76×10^{18}	4.76	7.90×10^{17}	1.01×10^{18}
Average of all dosimeters	3.36×10^7	1.23×10^{11}	4.13×10^{18}	4.76	8.68×10^{17}	1.01×10^{18}

TABLE 6-11

CALCULATED CURRENT AND EOL[a] VESSEL EXPOSURE FOR McGUIRE UNIT 1

Location	Calculated Current ϕ (E > 1.0 Mev) (n/cm^2)	Calculated EOL ϕ (E > 1.0 Mev) (n/cm^2)
Vessel IR	1.01×10^{18}	3.02×10^{19}
Vessel 1/4T	5.59×10^{17}	1.68×10^{19}
Vessel 3/4T	1.13×10^{17}	3.40×10^{18}

a. EOL fluences are based on operation at 3565 MWt for 32 EFPY

SECTION 7
SURVEILLANCE CAPSULE REMOVAL SCHEDULE

The following removal schedule is recommended for future capsules to be removed from the McGuire Unit 1 reactor vessel.

Capsule	Lead Factor	Removal Time[a]	Estimated Fluence ($n/cm^2 \times 10^{19}$)
U	4.76	Removed (1.06)	0.414 (Actual)
X	4.76	4	1.80[b]
V	4.06	8	3.07[c]
Y	4.06	15	5.75
W	4.76	Standby	--
Z	4.76	Standby	--

a. EFPY from plant startup

b. Approximates vessel end of life 1/4 thickness wall location fluence

c. Approximates vessel end of life inner wall location fluence

SECTION 8
REFERENCES

1. Davidson, J. A., and Yanichko, S.E., "Duke Power Company William B. McGuire Unit No. 1 Reactor Vessel Radiation Surveillance Program," WCAP-9195, November, 1977.

2. ASTM Standard E185-73, "Recommended Practice for Surveillance Tests for Nuclear Reactor Vessels" in ASTM Standards, Part 10 (1973), American Society for Testing and Materials, Philadelphia, 1973.

3. Regulatory Guide 1.99, Revision 1, "Effects of Residual Elements on Predicted Radiation Damage to Reactor Vessel Materials," U.S. Nuclear Regulatory Commission, April 1977.

4. Soltesz, R. G., Disney, R. K., Jedruch, J., and Zeigler, S.L., "Nuclear Rocket Shielding Methods, Modification, Updating and Input Data Preparation. Vol. 5 -- Two-Dimensional Discrete Ordinates Transport Technique," WANL-PR(LL)034, Vol. 5, August 1970.

5. SAILOR RSIC Data Library Collection DLC-76, "Coupled, Self-shielded, 47 Neutron, 20 Gamma-ray, P3, Cross Section Library for Light Water Reactors."

6. Benchmark Testing of Westinghouse Neutron Transport Analysis Methodology -- to be published.

7. ASTM Designation E261-77, Standard Practice for Measuring Neutron Flux, Fluence, and Spectra by Radioactivation Techniques," in ASTM Standards (1981), Part 45, Nuclear Standards, pp. 915-926, American Society for Testing and Materials, Philadelphia, 1[illegible]

8. ASTM Designation E262-77, "Standard Method for Measuring Thermal Neutron Flux by Radioactivation Techniques," in ASTM Standards (1981), Part 45, Nuclear Standards, pp. 927-935, American Society for Testing and Materials, Philadelphia, 1981.

9. ASTM Designation E263-77, "Standard Method for Measuring Thermal Neutron Flux by Radioactivation of Iron," in ASTM Standards (1981), Part 45, Nuclear Standards, pp. 936-941, American Society for Testing and Materials, Philadelphia, 1981.

10. ASTM Designation E481-78, "Standard Method for Measuring Neutron-Flux Density by Radioactivation of Cobalt and Silver," in ASTM Standards (1981), Part 45, Nuclear Standards, pp. 1063-1070, American Society for Testing and Materials, Philadelphia, 1981.

11. ASTM Designation E264-77, "Standard Method for Measuring Fast-Neutron Flux by Radioactivation of Nickel," in ASTM Standards (1981), Part 45, Nuclear Standards, pp. 942-945, American Society for Testing and Materials, Philadelphia, 1981.

APPENDIX A
HEATUP AND COOLDOWN LIMIT CURVES FOR NORMAL OPERATION

A-1. INTRODUCTION

Heatup and cooldown limit curves are calculated using the most limiting value of RT_{NDT} (reference nil-ductility temperature). The most limiting RT_{NDT} of the material in the core region of the reactor vessel is determined by using the preservice reactor vessel material properties and estimating the radiation-induced ΔRT_{NDT}. RT_{NDT} is designated as the higher of either the drop weight nil-ductility transition temperature (NDTT) or the temperature at which the material exhibits at least 50 ft-lb of impact energy and 35-mil lateral expansion (normal to the major working direction) minus 60°F.

RT_{NDT} increases as the material is exposed to fast-neutron radiation. Therefore, to find the most limiting RT_{NDT} at any time period in the reactor's life, ΔRT_{NDT} due to the radiation exposure associated with that time period must be added to the original unirradiated RT_{NDT}. The extent of the shift in RT_{NDT} is enhanced by certain chemical elements (such as copper and phosphorus) present in reactor vessel steels. Design curves which show the effect of fluence and copper and phosphorus contents on ΔRT_{NDT} for reactor vessel steels are shown in figure A-1.

Given the copper and phosphorus contents of the most limiting material, the radiation-induced ΔRT_{NDT} can be estimated from figure A-1. The most limiting material occurs in the lower shell longitudinal weld seam no. 3-442A listed in table A-1, and it is at an azimuthal angle of 60°. Fast neutron fluence (E > 1 Mev) for an azimuthal angle of 60° at the vessel inner surface, the 1/4 T (wall thickness), and 3/4 T (wall thickness) vessel locations are given as a function of full-power service life in figure A-2. The data for all other ferritic materials in the reactor coolant pressure boundary are examined to ensure that no other component will be limiting with respect to RT_{NDT}.

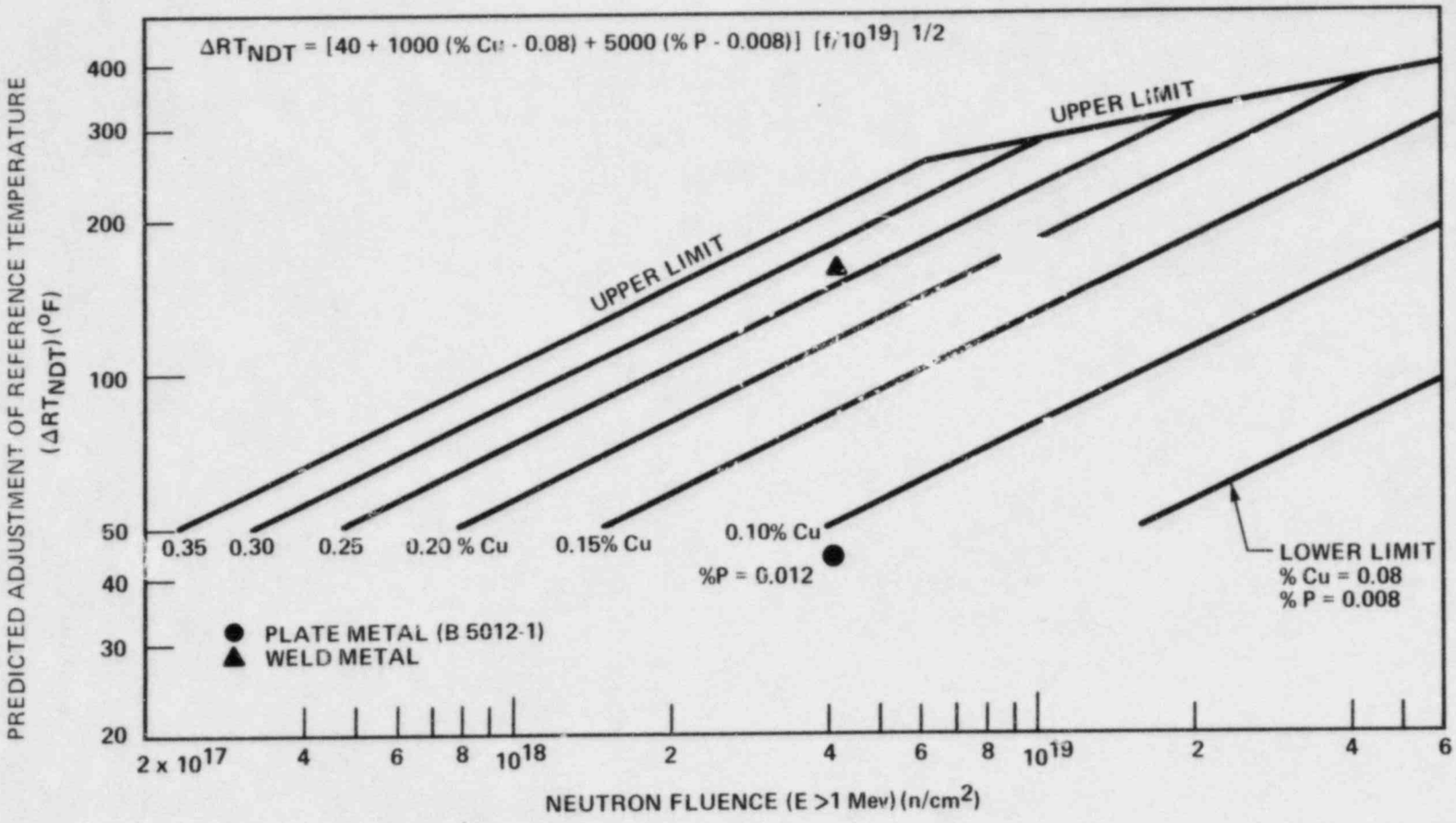

Figure A-1. Predicted Adjustment of Reference Temperature as a Function of Fluence, Copper, and Phosphorus Contents

12216-18

TABLE A-1

MCGUIRE UNIT 1 REACTOR VESSEL TOUGHNESS TABLE

Component	Material Specification Number	Code Number	Cu (%)	P (%)	Ni (%)	T_{NDT} (°F)	RT_{NDT} (°F)	USE (ft-lb)
Closure head dome	A533BCL.1	B5086-1	0.11	0.010	0.48	20	37[c]	65[c]
Closure head segments	A533BCL.1	B5087	0.11	0.008	0.62	10	10[c]	89[c]
Closure head flange	A508CL.2	B5002	--	0.010	0.75	40[c]	40[c]	101[c]
Vessel flange	A508CL.2	B4701	--	0.010	0.73	29[c]	29[c]	101[c]
Inlet nozzle	A508CL.2	B5003-1	0.12	0.010	0.68	60[c]	60[c]	89[c]
Inlet nozzle	A508CL.2	B5003-2	0.10	0.012	0.71	60[c]	60[c]	88[c]
Inlet nozzle	A508CL.2	B5003-3	0.10	0.009	0.69	60[c]	60[c]	79[c]
Inlet nozzle	A508CL.2	B5003-4	0.10	0.010	0.69	60[c]	60[c]	77[c]
Outlet nozzle	A508CL.2	B5004-1	--	0.005	0.74	60[c]	60[c]	82[c]
Outlet nozzle	A508CL.2	B5004-2	--	0.007	0.74	60[c]	60[c]	75[c]
Outlet nozzle	A508CL.2	B5004-3	--	0.005	0.71	60[c]	60[c]	90[c]
Outlet nozzle	A508CL.2	B5004-4	--	0.006	0.79	60[c]	60[c]	81[c]
Upper shell	A533BCL.1	B5453-2	0.14	0.011	0.58	10	15[c]	73[c]
Upper shell	A533BCL.1	B5011-2	0.10	0.011	0.54	10	27[c]	68[c]
Upper shell	A533BCL.1	B5011-3	0.13	0.010	0.56	0	0[c]	95[c]
Intermediate shell	A533BCL.1	B5012-1	0.13	0.010	0.60	-30	34	101
Intermediate shell	A533BCL.1	B5012-2	0.13	0.011	0.62	0	0	104.5
Intermediate shell	A533BCL.1	B5012-3	0.10	0.013	0.66	-20	-13	109
Lower shell	A533BCL.1	B5013-1	0.14	0.009	0.56	-10	0	94
Lower shell	A533BCL.1	B5013-2	0.10	0.010	0.52	-10	30	115
Lower shell	A533BCL.1	B5013-3	0.10	0.010	0.55	0	15	104
Bottom head segment	A533BCL.1	B5458-1	0.14	0.011	0.60	-70	-26[c]	90[c]
Bottom head segment	A533BCL.1	B5458-2	0.15	0.014	0.54	-30	-15[c]	96[c]
Bottom head segment	A533BCL.1	B5458-3	0.13	0.012	0.56	-20	2[c]	82[c]
Bottom head dome	A533BCL.1	B5085-1	0.13	0.010	0.53	0	10[c]	79[c]
Intermediate shell longitudinal weld seams	--	M1.22[a]	0.21	0.011	0.88	-60	-50	>110
Intermediate shell to lower shell weld	--	G1.39	0.05	0.006	--	-70	-70	>126
Lower shell longitudinal weld seams	--	M1.32	0.20	0.015	--	0[c]	0[c]	90
Lower shell longitudinal weld seams	--	M1.33[b]	0.21	0.016	0.68	0[c]	0[c]	--
Lower shell longitudinal weld seams	--	M1.34[b]	0.30	0.013	0.64	0[c]	0[c]	--

a. Used in reactor vessel surveillance weldment

b. Used in weld root region only

c. Estimated per U.S. NRC Standard Review Plan[1]

84858:1b-031985

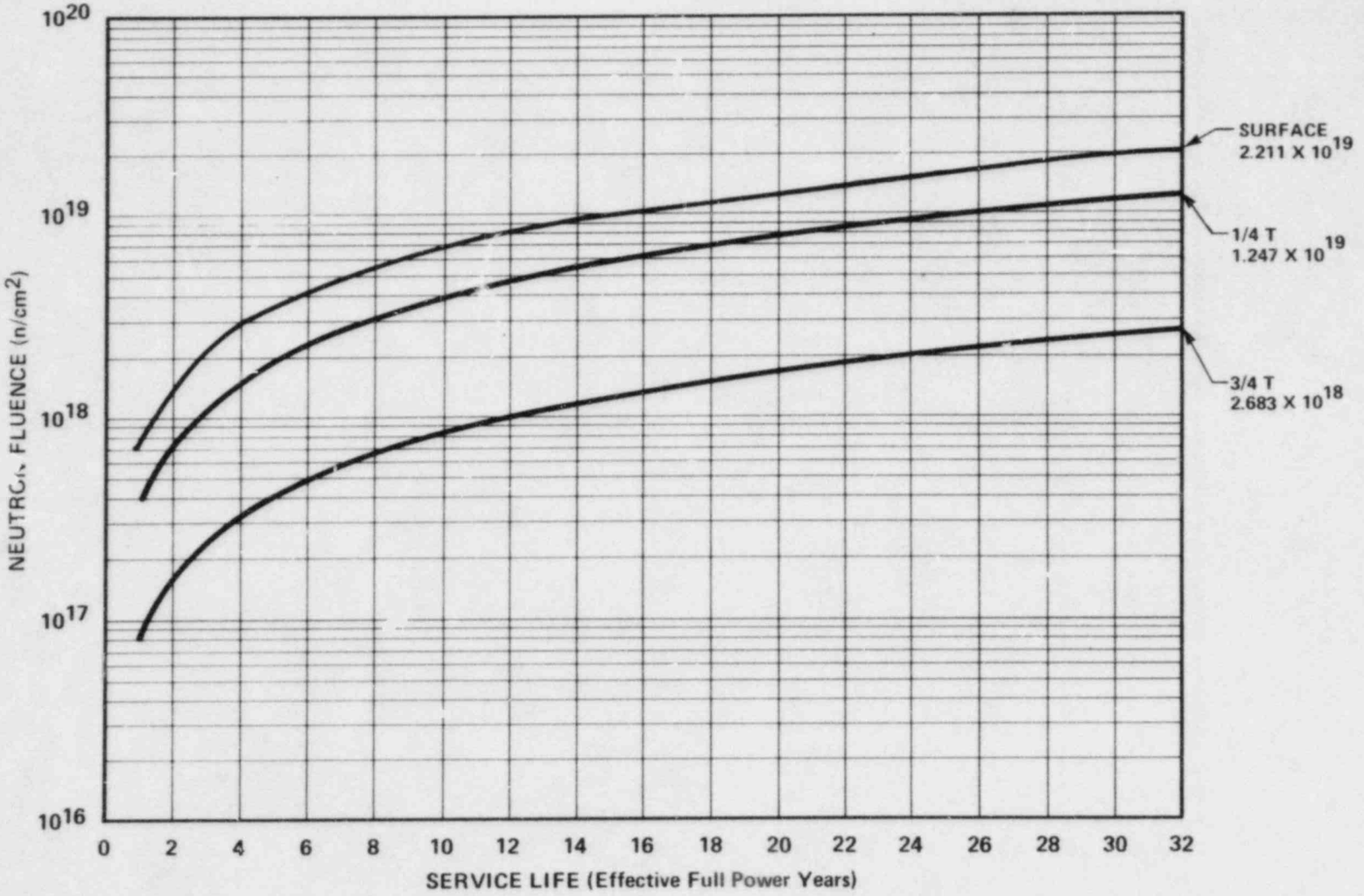

Figure A-2. Fast Neutron Fluence (E >1 Mev) as a Function of Full Power Service Life (EFPY)

12216-19

A-2. FRACTURE TOUGHNESS PROPERTIES

The preirradiation fracture-toughness properties of the McGuire Unit 1 reactor vessel materials are presented in table A-1. The fracture-toughness properties of the ferritic material in the reactor coolant pressure boundary are determined in accordance with the NRC Regulatory Standard Review Plan[1]. The postirradiation fracture-toughness properties of the reactor vessel beltline material were obtained directly from the McGuire Unit 1 Vessel Material Surveillance Program.

A-3. CRITERIA FOR ALLOWABLE PRESSURE-TEMPERATURE RELATIONSHIPS

The ASME approach for calculating the allowable limit curves for various heatup and cooldown rates specifies that the total stress intensity factor, K_I, for the combined thermal and pressure stresses at any time during heatup or cooldown cannot be greater than the reference stress intensity factor, K_{IR}, for the metal temperature at that time. K_{IR} is obtained from the reference fracture toughness curve, defined in Appendix G to the ASME Code.[2] The K_{IR} curve is given by the following equation.

$$K_{IR} = 26.78 + 1.223 \exp [0.0145 (T-RT_{NDT} + 160)] \qquad (A-1)$$

where

K_{IR} = reference stress intensity factor as a function of the metal temperature T and the metal reference nil-ductility temperature RT_{NDT}

Therefore, the governing equation for the heatup-cooldown analysis is defined in Appendix G of the ASME Code[2] as follows.

$$C K_{IM} + K_{It} \leq K_{IR} \qquad (A-2)$$

where

K_{IM} = stress intensity factor caused by membrane (pressure) stress

K_{It} = stress intensity factor caused by the thermal gradients

K_{IR} = function of temperature relative to the RT_{NDT} of the material

C = 2.0 for Level A and Level B service limits

C = 1.5 for hydrostatic and leak test conditions during which the reactor core is not critical

At any time during the heatup or cooldown transient, K_{IR} is determined by the metal temperature at the tip of the postulated flaw, the appropriate value for RT_{NDT}, and the reference fracture toughness curve. The thermal stresses resulting from temperature gradients through the vessel wall are calculated and then the corresponding (thermal) stress intensity factors, K_{It}, for the reference flaw are computed. From equation A-2, the pressure stress intensity factors are obtained and, from these, the allowable pressures are calculated.

For the calculation of the allowable pressure versus coolant temperature during cooldown, the reference flaw of Appendix G to the ASME Code is assumed to exist at the inside of the vessel wall. During cooldown, the controlling location of the flaw is always at the inside of the wall because the thermal gradients produce tensile stresses at the inside, which increase with increasing cooldown rates. Allowable pressure-temperature relations are generated for both steady-state and finite cooldown rate situations. From these relations, composite limit curves are constructed for each cooldown rate of interest.

The use of the composite curve in the cooldown analysis is necessary because control of the cooldown procedure is based on measurement of reactor coolant temperature, whereas the limiting pressure is actually dependent on the material temperature at the tip of the assumed flaw.

During cooldown, the 1/4 T vessel location is at a higher temperature than the fluid adjacent to the vessel ID. This condition, of course, is not true for the steady-state situation. It follows that, at any given reactor coolant temperature, the ΔT developed during cooldown results in a higher value of K_{IR} at the 1/4 T location for finite cooldown rates than for steady-state operation. Furthermore, if conditions exist so that the increase in K_{IR} exceeds K_{It}, the calculated allowable pressure during cooldown will be greater than the steady-state value.

The above procedures are needed because there is no direct control on temperature at the 1/4 T location and, therefore, allowable pressures may unknowingly be violated if the rate of cooling is decreased at various intervals along a cooldown ramp. The use of the composite curve eliminates this problem and ensures conservative operation of the system for the entire cooldown period.

Three separate calculations are required to determine the limit curves for finite heatup rates. As is done in the cooldown analysis, allowable pressure-temperature relationships are developed for steady-state conditions as well as finite heatup rate conditions assuming the presence of a 1/4 T defect at the inside of the vessel wall. The thermal gradients during heatup produce compressive stresses at the inside of the wall that alleviate the tensile stresses produced by internal pressure. The metal temperature at the crack tip lags the coolant temperature; therefore, the K_{IR} for the 1/4 T crack during heatup is lower than the K_{IR} for the 1/4 T crack during steady-state conditions at the same coolant temperature. During heatup, especially at the end of the transient, conditions may exist so that the effects of compressive thermal stresses and lower K_{IR}'s do not offset each other, and the pressure-temperature curve based on steady-state conditions no longer represents a lower bound of all similar curves for finite heatup rates when the 1/4 T flaw is considered. Therefore, both cases have to be analyzed in order to ensure that at any coolant temperature the lower value of the allowable pressure calculated for steady-state and finite heatup rates is obtained.

The second portion of the heatup analysis concerns the calculation of pressure-temperature limitations for the case in which a 1/4 T deep outside surface flaw is assumed. Unlike the situation at the vessel inside surface, the thermal gradients established at the outside surface during heatup produce stresses which are tensile in nature and therefore tend to reinforce any pressure stresses present. These thermal stresses are dependent on both the rate of heatup and the time (or coolant temperature) along the heatup ramp. Since the thermal stresses at the outside are tensile and increase with increasing heatup rates, each heatup rate must be analyzed on an individual basis.

Following the generation of pressure-temperature curves for both the steady-state and finite heatup rate situations, the final limit curves are produced by constructing a composite curve based on a point-by-point comparison of the steady-state and finite heatup rate data. At any given temperature, the allowable pressure is taken to be the lesser of the three values taken from the curves under consideration. The use of the composite curve is necessary to set conservative heatup limitations because it is possible for conditions to exist wherein, over the course of the heatup ramp, the controlling condition switches from the inside to the outside and the pressure limit must at all times be based on analysis of the most critical criterion. Then, composite curves for the heatup rate data and the cooldown rate data are adjusted for possible errors in the pressure and temperature sensing instruments by the values indicated on figures A-3 and A-4.

Finally, the new 10CFR50[3] rule which addresses the metal temperature of the closure head flange and vessel flange regions is considered. This 10CFR50 rule states that the metal temperature of the closure flange regions must exceed the material RT_{NDT} by at least 120°F for normal operation when the pressure exceeds 20 percent of the preservice hydrostatic test pressure (621 psig for McGuire Unit 1). Table A-1 indicates that the limiting RT_{NDT} of 40°F occurs in the closure head flange of McGuire Unit 1, and the minimum allowable temperature of this region is 160°F at pressures greater than 621 psig.

12216-20

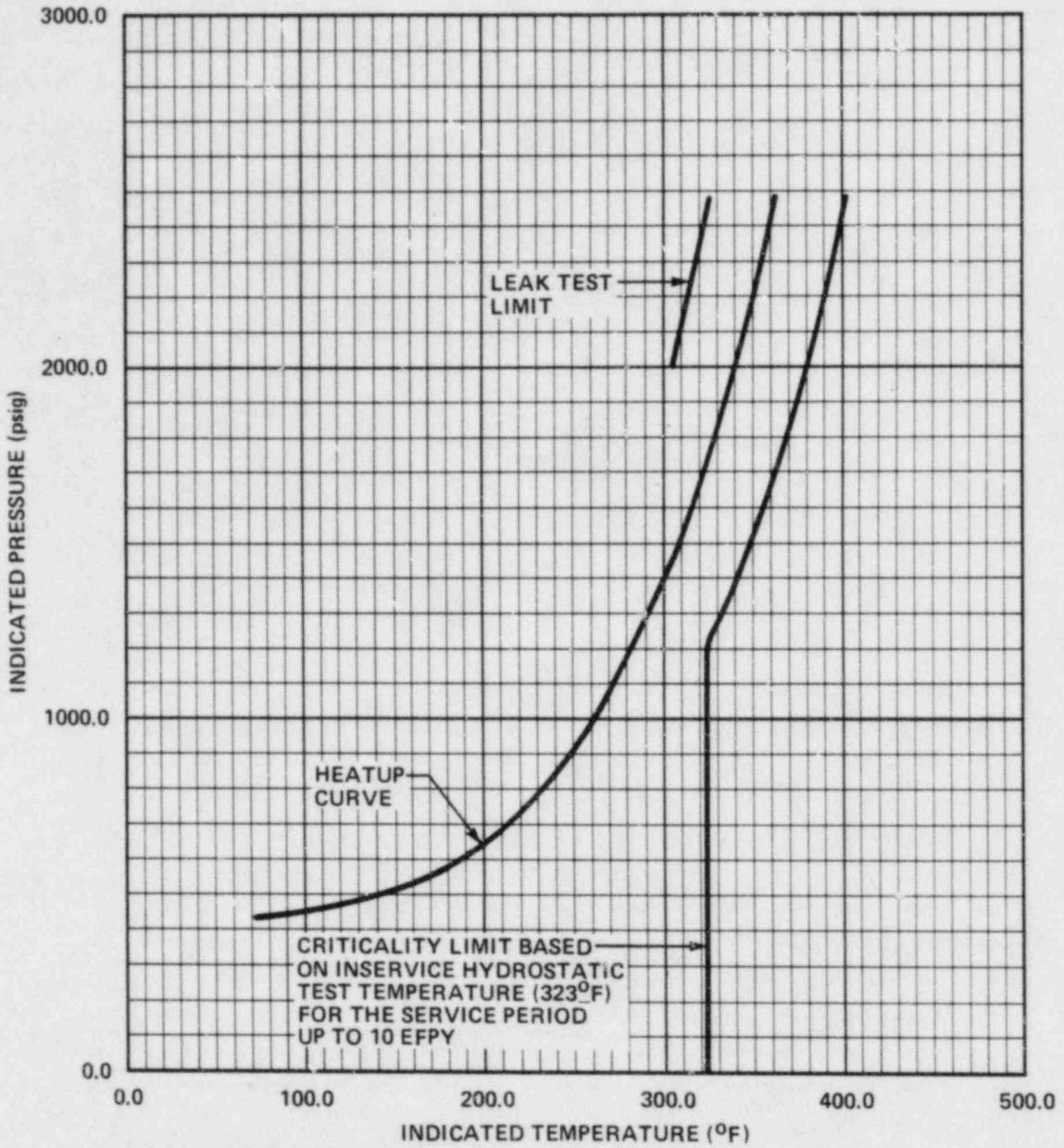

MATERIAL PROPERTY BASIS

CONTROLLING MATERIAL	: WELD METAL
COPPER CONTENT	: 0.30 wt%
PHOSPHORUS CONTENT	: 0.013 wt%
RT_{NDT} INITIAL	: 0°F
RT_{NDT} AFTER 10 EFPY	: 1/4T, 178°F
	: 3/4, 83°F

CURVE APPLICABLE FOR HEATUP RATES UP TO 60°F/HR FOR THE SERVICE PERIOD UP TO 10 EFPY AND CONTAINS MARGINS OF 10°F AND 60 PSIG FOR POSSIBLE INSTRUMENT ERRORS.

Figure A-3. McGuire Unit 1 Reactor Coolant System Heatup Limitations Applicable for the First 10 EFPY

12216-21

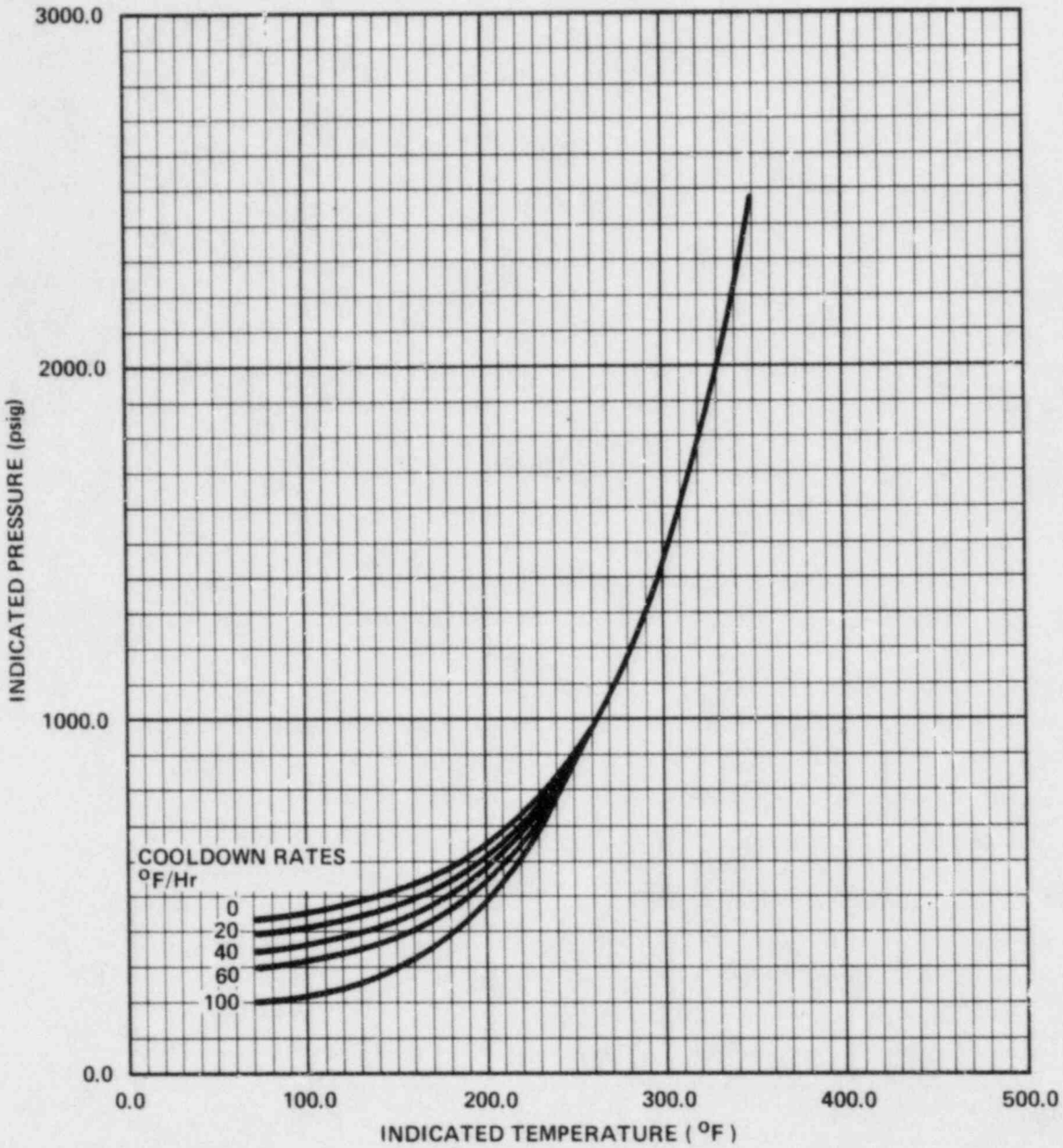

MATERIAL PROPERTY BASIS

CONTROLLING MATERIAL	: WELD METAL
COPPER CONTENT	: 0.30 wt%
PHOSPHORUS CONTENT	: 0.013 wt%
RT_{NDT} INITIAL	: 0°F
RT_{NDT} AFTER 10 EFPY	: 1/4, 178°F
	: 3/4, 83°F

CURVES APPLICABLE FOR COOLDOWN RATES UP TO 100°F/HR FOR THE SERVICE PERIOD UP TO 10 EFPY AND CONTAINS MARGINS OF 10°F AND 60 PSIG FOR POSSIBLE INSTRUMENT ERRORS.

Figure A-4. McGuire Unit 1 Reactor Coolant System Cooldown Limitations Applicable for the First 10 EFPY

A-4. HEATUP AND COOLDOWN LIMIT CURVES

Limit curves for normal heatup and cooldown of the primary Reactor Coolant System have been calculated using the methods discussed in section A-3. The derivation of the limit curves is presented in the NRC Regulatory Standard Review Plan.[4]

Transition temperature shifts occurring in the pressure vessel materials due to radiation exposure have been obtained directly from the reactor pressure vessel surveillance program. Charpy test specimens from Capsule U indicate that the surveillance weld metal and limiting core region intermediate shell plate heat no. B5012-1 exhibited shifts in RT_{NDT} of 160°F and 45°F, respectively. These shifts at a fluence of 4.14×10^{18} n/cm^2 are well within the appropriate design curve (figure A-1) prediction. As a result, the heatup and cooldown curves are based on the ΔRT_{NDT} given in figure A-1 for the most limiting beltline material which is in the lower shell longitudinal weld seam no. 3-442A. The resultant heatup and cooldown limit curves for normal operation of the reactor vessel are presented in figures A-3 and A-4 and represent an operational time period of 10 EFPY. These limit curves are not impacted by the new 10CRF50 rule.

Allowable combinations of temperature and pressure for specific temperature change rates are below and to the right of the limit lines shown on the heatup and cooldown curves. The reactor must not be made critical until pressure-temperature combinations are to the right of the criticality limit line shown in figure A-3. This is in addition to other criteria which must be met before the reactor is made critical.

The leak test limit curve shown in figure A-3 represents minimum temperature requirements at the leak test pressure specified by applicable codes. The leak test limit curve was determined by methods of references 2 and 4.

Figures A-3 and A-4 define limits for ensuring prevention of nonductile failure.

APPENDIX A
REFERENCES

1. "Fracture Toughness Requirements," Branch Technical Position MTEB 5-2, Chapter 5.3.2 in Standard Review Plan for the Review of Safety Analysis Reports for Nuclear Power Plants, LWR Edition, NUREG-0800, 1981.

2. ASME Boiler and Pressure Vessel Code, Section III, Division 1 - Appendices, "Rules for Construction of Nuclear Vessels," Appendix G, "Protection Against Nonductile Failure," pp. 559-564, 1983 Edition, American Society of Mechanical Engineers, New York, 1983.

3. Code of Federal Regulations, 10CFR50, Appendix G, "Fracture Toughness Requirements," U.S. Nuclear Regulatory Commission, Washington, D.C., Amended May 17, 1983 (48 Federal Register 24010).

4. "Pressure-Temperature Limits," Chapter 5.3.2 in Standard Review Plan for the Review of Safety Analysis Reports for Nuclear Power Plants, LWR Edition, NUREG-0800, 1981.